

1 **Tandemly duplicated *MYB* genes specifically in the Phaseoleae lineage are**
2 **functionally diverged in the regulation of anthocyanin biosynthesis**

3 Ruirui Ma¹, Wenzuan Huang¹, Quan Hu¹, Guo Tian¹, Jie An¹, Ting Fang¹, Jia Liu¹,
4 Jingjing Hou¹, Meixia Zhao^{2*}, Lianjun Sun^{1*}

5 ¹ College of Agronomy and Biotechnology, China Agricultural University, Beijing
6 100193, China

7 ² Department of Microbiology and Cell Science, University of Florida, Gainesville,
8 FL 32611, USA

9 * Correspondences: Lianjun Sun (sunlj@cau.edu.cn); Meixia Zhao
10 (meixiazhao@ufl.edu)

11

12 **Abstract**

13 Gene duplications have long been recognized as a driving force in the evolution of
14 genes, giving rise to novel functions. The soybean genome is characterized by a large
15 extent of duplicated genes. However, the extent and mechanisms of functional
16 divergence among these duplicated genes in soybean remain poorly understood. In
17 this study, we revealed that tandem duplication of *MYB* genes, which occurred
18 specifically in the Phaseoleae lineage, exhibited a stronger purifying selection in
19 soybean compared to common bean. To gain insights into the diverse functions of
20 these *MYB* genes in anthocyanin biosynthesis, we examined the expression,
21 transcriptional activity, metabolite, and evolutionary history of four *MYB* genes
22 (*GmMYBA5*, *GmMYBA2*, *GmMYBA1* and *Glyma.09g235000*), which were
23 presumably generated by tandem duplication in soybean. Our data revealed that
24 *Glyma.09g235000* had become a pseudogene, while the remaining three *MYB* genes
25 exhibited strong transcriptional activation activity and promoted anthocyanin
26 biosynthesis in different soybean tissues. Furthermore, *GmMYBA5* produced distinct
27 compounds in *Nicotiana benthamiana* leaves compared to *GmMYBA2* and *GmMYBA1*
28 due to variations in their DNA binding domains. The lower expression of anthocyanin
29 related genes in *GmMYBA5* resulted in lower levels of anthocyanins compared to

30 *GmMYBA2* and *GmMYBA1*. Metabolomics analysis further demonstrated the diverse
31 and differential downstream metabolites, suggesting their functional divergence in
32 metabolites following gene duplication. Together, our data provided evidence of
33 functional divergence within the *MYB* gene cluster following tandem duplication,
34 which shed light on the potential evolutionary direction of gene duplications during
35 legume evolution.

36 **Keywords:** tandemly duplicated *MYB* genes, anthocyanins, functional divergence,
37 metabolites, legume

38 **Introduction**

39 In flowering plants, polyploidy or whole-genome duplication is a key process that
40 leads to gene duplication, which provide genetic resources for generating functional
41 novelty (Soltis et al., 2015; Soltis and Soltis, 2016). In addition to polyploidy, another
42 two important processes that result in an increase in gene copy number are segmental
43 and tandem duplication (Rizzon et al., 2006; Freeling, 2009). Following duplication
44 events, duplicated genes undergo functional divergence, which can occur through
45 pseudogenization resulting in loss of function, neofunctionalization leading to the
46 acquisition of novel functions, or subfunctionalization where the duplicated genes
47 retain partial functions of the ancestor gene (Sandve et al., 2018). The phenomenon of
48 functional divergence in duplicated genes has been observed in many species. For
49 instance, in citrus, the *Ruby2–Ruby1* gene cluster exhibits subfunctionalization, with
50 these two genes exerting opposite effects in the regulation of anthocyanin
51 biosynthesis (Huang et al., 2018). In maize, the duplicated *MYB* genes, *P1* and *P2*,
52 show different expression patterns that contribute to tissue-specific pigmentation
53 (Zhang et al., 2000). In *Solanum commersonii*, the tandem paralogs *ScAN1* and *ScAN2*
54 have diverged in function with one gene specialized in anthocyanin production and
55 the other one maintaining the conserved function of responding to cold stress
56 (D'Amelia et al., 2018). These examples clearly demonstrate the functional divergence
57 of genes following duplication events. Soybean, which has undergone two polyploidy
58 events, has experienced substantial tandem duplication events, resulting in a

59 significant expansion of genes involved in the anthocyanin biosynthetic pathway
60 (Kim et al., 2012).

61 Anthocyanins, one of the largest groups of plant flavonoid compounds, not only
62 confer appealing colors to plants but also contribute their tolerance to biotic and
63 abiotic stresses, including drought, cold, ultraviolet (UV)-B, heavy metals, herbivores,
64 and pathogens (Gould, 2004; Hichri et al., 2011; Kovinich et al., 2015). Moreover,
65 anthocyanins offer human health benefits to by protecting against chronic diseases
66 such as metabolic syndrome, cardiovascular disease, and certain cancers (Zhang *et al.*,
67 2014; Putta et al., 2017). The biosynthesis of anthocyanins stems from the general
68 phenylpropanoid pathway and involves several catalytic enzymes, including chalcone
69 synthase (CHS), chalcone isomerase (CHI), flavanone 3-hydroxylase (F3H),
70 flavonoid 3'hydroxylase (F3'H), flavonoid 3'5' hydroxylase (F3'5'H),
71 dihydroflavonol 4-reductase (DFR), anthocyanidin synthase (ANS), and
72 UDP-flavonoid glucosyltransferase (UFGT) (Sundaramoorthy et al., 2015; Xu et al.,
73 2015) (Supplementary Fig. S1). The expression of anthocyanin biosynthetic genes is
74 primarily regulated by the MYB-bHLH (helix-loop-helix)-WD repeat (MBW)
75 transcriptional complex (Albert et al., 2014; Lloyd et al., 2017; Wang et al., 2021;
76 Wang et al., 2022). The critical part of the MBW transcriptional complex is MYB
77 transcription factors, which are the key determinants of pigmentation and have been
78 identified in various crops such as maize, rice, wheat and foxtail millet (Grotewold et
79 al., 1994; Chin et al., 2016; Shin et al., 2016; Li et al., 2022b). Specific patterns and
80 spatial localizations of anthocyanins determined by MYB transcription factors have
81 also been reported in apple, snapdragon, petunia and lily (Liu et al., 2015). However,
82 limited research has focused on the diverse metabolites and anthocyanin components,
83 which play distinct roles in environmental adaptation produced by tandemly
84 duplicated *MYB* genes.

85 Soybean (*Glycine max* (L.) Merr.) is one of the world's most important legume
86 crops that provides plant protein, oil and other essential ingredients for humans and
87 livestock (Malle et al., 2020). Compared to its wild relative *Glycine soja* (Sieb. &
88 Zucc.), cultivated soybean and landraces exhibit a wide range of morphological types

89 in order to meet human needs (Li et al., 2008). Various parts of the soybean plant,
90 including hypocotyls, petioles, flowers, and seeds display significant natural variation
91 in color due to distinct accumulation and distribution patterns of anthocyanins and
92 proanthocyanins (Jeong et al., 2019; Xie et al., 2019). Previous studies have shown
93 that the loss of anthocyanin pigment in cereals during domestication, diversification,
94 and improvement is controlled by the same *MYB* gene (Li et al., 2022b). However,
95 only a limited number of transcription factors responsible for anthocyanins
96 biosynthesis have been studied in legume (Lu et al., 2021). The function and
97 evolutionary history of syntenic block in legume is unknown. Therefore, it is crucial
98 to investigate the mechanisms underlying the molecular mechanisms and functional
99 divergence of tandemly duplicated *MYB* transcription factors in the regulation of
100 anthocyanin biosynthesis in legumes.

101 Previous studies have described the collinear region of the *MYB* transcription
102 factors cluster in legumes, which conservatively contributed to seed coat color in
103 soybean, common bean and cowpea (Zabala et al., 2014; García-Fernández et al.,
104 2021; Herniter et al., 2018). In this study, we revealed the tandemly duplicated *MYB*
105 gene cluster that emerged prior to the divergence of soybean from other legume
106 species during the common legume tetraploidy event. We observed a stronger
107 purifying selection acting on this cluster in soybean. With the exception of one
108 pseudogene (*Glyma.09g235000*), all duplicated genes exhibited the potential to
109 activate anthocyanin biosynthesis with tissue-specific patterns. Through ectopic
110 expression and metabolomics analysis, we found that the *MYB* genes exhibited
111 functional divergence in activation activities and specificity of downstream target
112 catalytic enzymes, and metabolites. Additionally, a domain swap experiment
113 suggested the divergent R2R3 DNA binding domain primary accounted for the
114 distinct phenotype observed in *GmMYBA5*. Metabolomics analysis further
115 demonstrated the diverse and differential downstream metabolites, suggesting their
116 functional divergence in metabolites following gene duplication. Taken together, our
117 findings shed light on the characteristics of functional divergence within a *MYB* gene
118 cluster, and provide new insights into the evolutionary history of gene duplications

119 and functional divergence as a mechanism driving adaptation during legume
120 evolution.

121 **Results**

122 **Tandem duplication of the *MYB* genes occurs specifically in the Phaseoleae
123 lineage and exhibits a stronger purifying selection in soybean**

124 Soybean has undergone two polyploidy events and substantial tandem duplication
125 events, resulting in a significant expansion of duplicated regions and genes involved
126 in the regulation of anthocyanin biosynthesis, specifically the *MYB* transcription
127 factors (Kim et al., 2012). The *R* locus (*GmMYBA2*, *Glyma.09g235100*), is an R2R3
128 *MYB* activator located on chromosome 9. It is flanked by three tandemly duplicated
129 *MYB* genes: *GmMYBA5* (*Glyma.09g234900*), *GmMYBA1* (*Glyma.09g235300*) and
130 *Glyma.09g235000* (Gao et al., 2021) (Fig. 1A). *Glyma.09g235000* was identified as a
131 pseudogene due to its lack of expression in any soybean tissue (Gillman et al., 2011).
132 To shed light on the evolutionary forces driving the divergence of the *MYB* genes, we
133 analyzed a region containing the *MYB* gene cluster in different legumes genomes,
134 which have been known to contributed conservatively to seed coat color in soybean,
135 common bean, and cowpea (Zabala et al., 2014; García-Fernández et al., 2021;
136 Herniter et al., 2018). The results indicated that the numbers of tandemly duplicated
137 *MYB* genes varied across different species (Fig. 1B). In certain species such as
138 *Trifolium pratense*, *Cicer arietinum*, *Pisum sativum* and *Aeschynomene evenia*, which
139 diverged earlier from the legume common tetraploidy event, there was only a single
140 copy of the *MYB* transcription factor gene in the collinear regions (Wang et al., 2017).
141 However, an increased number of *MYB* genes was observed in the genera of
142 *phaseolus* and *vigna*, which diverged from soybean approximately 27.3 million years
143 ago (MYA). Notably, we detected four homologous genes in the syntenic region of
144 common bean (*Phaseolus vulgaris*) (Fig. 1B). Interestingly, although all four
145 homologous genes were present, the best matches for *GmMYBA5*, *GmMYBA2* and
146 *GmMYBA1* in common bean were found to be *Phvul.008G038200*. To further explore
147 the evolutionary divergence of these three soybean *MYB* genes, we next compared

148 the evolutionary distance of the three soybean *MYB* genes using common bean as an
149 outgroup. Our data revealed that ω (Ka/Ks, where Ka represents nonsynonymous
150 substitution and Ks represents synonymous substitution) for *GmMYBA5* was higher
151 than that of *GmMYBA2* and *GmMYBA1* (Table 1), suggesting that *GmMYBA5* has
152 experienced a lower intensity of purifying selection compared to the other two genes.
153 Furthermore, our data indicated that the *MYB* genes in soybean exhibited lower rates
154 of substitution for both Ka and Ks when compared to common bean, consistent with
155 the genome-wide analysis of all genes between soybean and common bean (Zhao et
156 al., 2017). Intriguingly, despite the significantly higher ω observed at the
157 genome-wide level in soybean (Zhao et al., 2017), a lower ω was observed specially
158 for these *MYB* genes in soybean, suggesting that the *MYB* genes have undergone a
159 stronger purifying selection in soybean after their split with common bean.

160 It is worth noting that our data revealed that the soybean specific whole-genome
161 duplication (13 MYA) did not significantly increase the number of tandemly
162 duplicated genes in this region. Instead, it led to an increase in the number of
163 homoeologous genes within the duplicated region on chromosome 18 (Fig. 1B).
164 Interestingly, while the homoeologous genes of *GmMYBA2* and *GmMYBA1* on
165 chromosome 18 were retained, the homoeologous gene of *GmMYBA5* was lost, likely
166 occurring subsequent to the whole-genome duplication event. Taken together, our data
167 suggest that the *MYB* gene cluster originated through tandem duplication prior to the
168 soybean specific whole-genome duplication and *GmMYBA5* has undergone greater
169 functional divergence. Anthocyanins, as important metabolites, are often induced by
170 environmental stresses in plants (Li et al., 2022b). The increased number of *MYB*
171 genes in different legumes may represent an adaptive strategy for these plants to
172 respond to diverse external environmental conditions.

173 **Tandemly duplicated *MYB* genes are putative anthocyanin synthesis regulators**

174 The identification of *Glyma.09g235000* as a pseudogene (Gillman et al., 2011)
175 prompted us to further investigate its function. To further confirm its role, we
176 performed the ectopic expression of the coding sequence of *Glyma.09g235000* driven
177 by the 35S promoter of cauliflower mosaic virus (CaMV) in *Arabidopsis thaliana*.

178 However, no phenotypic differences were observed in pigmentation between the
179 transgenic plants and the wild types, indicating the loss of its regulatory function in
180 anthocyanin synthesis (Supplementary Fig. S2). Therefore, we focused on the
181 molecular function of the remaining three genes. Alignment of the amino acid
182 sequences showed an 86.58% similarity among *GmMYBA5*, *GmMYBA2* and
183 *GmMYBA1*. These three genes all contained the conserved R2 and R3 repeats, as well
184 as the [D/E]Lx2[R/ K]x3Lx6Lx3R domain, which interacts with the R/B-like bHLH
185 proteins (Supplementary Fig. S3). In addition, the conserved motif KPRPR[S/T] [F/L],
186 which is important for anthocyanin activation, were present in all three genes (Stracke
187 et al., 2001) (Fig. 2A). To elucidate the evolutionary relationship of these *MYB* genes,
188 a phylogenetic tree was constructed using the protein sequences of known
189 anthocyanin and proanthocyanin related *MYB* regulators from *Arabidopsis*, *Medicago*
190 and *Vinifera*. The phylogenetic analysis classified these homologous genes into two
191 major groups “anthocyanin activator” and “proanthocyanin activator”. Notably, all of
192 the three *MYB* genes from the cluster fell within the “anthocyanin activator” group,
193 indicating their potential roles in anthocyanin biosynthesis (Fig. 2B).

194 ***GmMYBA5*, *GmMYBA2* and *GmMYBA1* are transcription factors that can
195 activate anthocyanin biosynthesis**

196 The subcellular distribution of *GmMYBA5*, *GmMYBA2* and *GmMYBA1* was
197 investigated by expressing fusion protein of these genes with green fluorescent
198 protein (GFP) in tobacco (*Nicotiana benthamiana*) leaf epidermal cells. The GFP
199 fluorescent signals were observed specifically in the nuclei of all of the three genes
200 (Fig. 3A), indicating that these genes are localized in the nucleus. To access their
201 transcriptional activity, the full coding sequences of *GmMYBA5*, *GmMYBA2* and
202 *GmMYBA1* were fused with the GAL4 DNA binding domain of yeast in the
203 expression vector pGBKT7. The results showed that yeast transformants carrying
204 these constructs were able to grow on medium lacking Trp, His and Ade, indicating
205 that these three genes function as transcription factors with robust transcriptional
206 activity (Fig. 3B). Furthermore, we introduced overexpression constructs containing
207 the coding sequences of *GmMYBA5*, *GmMYBA2* and *GmMYBA1* driven by the 35S

208 promoter of cauliflower mosaic virus (CaMV) into *Arabidopsis thaliana*. Compared
209 to the wild type control, all five independent T₂ transgenic lines exhibited purple
210 pigment accumulation in various tissues, including seedlings, leaves, roots, and leaf
211 veins (Fig. 3C and Supplementary Fig. S4). These findings demonstrate that
212 *GmMYBA5*, *GmMYBA2* and *GmMYBA1* are nucleus-localized transcription factors
213 with strong transcriptional activity that can activate the anthocyanin biosynthesis in
214 vivo.

215 **Functional divergence of *GmMYBA5*, *GmMYBA2* and *GmMYBA1***

216 Previous studies have reported the specific expression pattern of *GmMYBA2* in the
217 seed coat (Gillman et al., 2011). To validate this, quantitative reverse transcriptase
218 (RT)-PCR analysis was performed on various soybean tissues, including stems, leaves,
219 pods, and seeds. Consistent with previous findings, *GmMYBA2* was specifically
220 expressed in seeds. Conversely, *GmMYBA5* was primarily expressed in vegetative
221 tissues such as stems, leaves, and pods. In contrast, *GmMYBA1* displayed low
222 expression levels restricted to leaves and stems (Fig. 4A). To further investigate the
223 impact of ectopic expression of these three genes, transient overexpression of these
224 three genes were conducted in *Nicotiana benthamiana* leaves. Leaves overexpressing
225 *GmMYBA5*, *GmMYBA2* and *GmMYBA1* exhibited a noticeable
226 anthocyanin-pigmented phenotype, and the anthocyanin content was significantly
227 higher compared to the leaves with an empty vector control (Fig. 4B and C).
228 Interestingly, the anthocyanin solution extracted from leaves overexpressing
229 *GmMYBA5* displayed a brownish color instead of the purple color observed in leaves
230 overexpressing *GmMYBA2* and *GmMYBA1* (Fig. 4B). This observation suggests that
231 the ectopic expression of *GmMYBA5*, *GmMYBA2* and *GmMYBA1* leads to the
232 production of distinct metabolites in *Nicotiana benthamiana* leaves.

233 To elucidate the molecular basis underlying these different metabolites, domain
234 swap experiments were performed. The DNA binding domains (BD; corresponding to
235 R2R3 domain) and the activating domains (AD; corresponding to C-terminal domain)
236 of *GmMYBA5*, *GmMYBA2* and *GmMYBA1* were exchanged, generating chimeric
237 proteins (Fig. 5A). Our results showed that when the BD of *GmMYBA5* was fused

238 with the AD of either *GmMYBA2* or *GmMYBA1*, the resulting chimeric proteins
239 retained the phenotype of *GmMYBA5* (Fig. 5B). This indicates that the unique
240 brownish metabolites produced by *GmMYBA5* is primarily influenced by its divergent
241 R2R3 domains and potentially by its binding ability.

242 Additional experiments were performed in soybean hair roots to further investigate
243 the function of the MYB genes. The highly expressed GmScreamM4 promoter (pM4)
244 was utilized to replace 35S promoter of the plant expression vector pTF101, (Zhang et
245 al., 2015), and the full coding sequences of *GmMYBA5*, *GmMYBA2* and *GmMYBA1*
246 were inserted. These constructs were transformed into *Agrobacterium rhizogenes*
247 K599, and soybean cotyledons were infected to generate transgenic soybean hairy
248 roots. Transgenic soybean hairy roots carrying the three genes exhibited purple
249 pigmentation in some roots, with the pM4:*GmMYBA5* transgenic soybean hairy roots
250 displaying less pigmentation compared to the others (Fig. 5C). Expression analysis
251 revealed that the expression levels of catalytic enzymes genes, including *GmF3H*,
252 *GmF3'H*, *GmF3'5'H*, *GmDFR1*, *GmDFR2*, *GmANS1*, *GmANS2*, *GmUGT78K1*, and
253 *GmUGT78K2*, were significantly upregulated in the overexpression lines, although to
254 a lesser extent in *GmMYBA5* lines compared to the other lines (Fig. 5D). These results
255 suggest that *GmMYBA5* has a lower capacity to activate catalytic genes involved in
256 anthocyanin biosynthesis, resulting in reduced visible anthocyanin accumulation in
257 roots. Overall, our data demonstrate that these tandemly duplicated *MYB* genes have
258 undergone functional divergence, leading to tissue-specific expression patterns and
259 differential activation abilities for anthocyanin biosynthesis.

260 **Metabolomics analysis of metabolites produced by *GmMYBA5*, *GmMYBA2* and
261 *GmMYBA1***

262 To gain further insights into the functionality of the three *MYB* genes, we examined
263 the downstream compounds in soybean hairy roots overexpressing pM4:*GmMYBA5*,
264 pM4:*GmMYBA2* and pM4:*GmMYBA1*, as well as control roots with an empty vector,
265 using Liquid Chromatograph Mass Spectrometer (LC-MS). In total, we identified 156
266 flavonoid compounds across all samples, with 80 (51.3%) belonging to flavones and
267 flavonols, 30 (19.2%) classified as isoflavonoids, and 12 (7.7%) identified as

268 anthocyanins (Fig. 6A and Supplementary Table S1). To ensure the reliability of the
269 metabolite extraction and detection, we assessed the total ion flow diagram (TIC) of
270 the mass spectrometry analysis and calculated the Pearson correlation coefficient for
271 different quality control (QC) samples. Our data demonstrated a high correlation,
272 indicating the repeatability of both metabolite extraction and detection
273 (Supplementary Fig. S5A and B). Furthermore, we performed principal component
274 analysis (PCA) and hierarchical clustering to evaluate the biological repeatability
275 among the samples. The PCA score plot and hierarchical clustering heatmap clearly
276 revealed that all samples were distinctly separated into the four expected groups,
277 affirming the high quality and repeatability of the data (Supplementary Figs. S5C and
278 S6).

279 The abundances of the 156 metabolic compounds were compared between the
280 overexpression groups of the three genes and the control group with empty vectors, as
281 well as within the overexpression groups. Differential metabolites were defined as
282 those meeting the threshold criteria of $p \leq 0.05$ (Student's t test) and $|\log_2\text{FC} (\text{Fold}$
283 $\text{Change})| \geq 1$. Our analysis revealed that the overexpression of *GmMYBA2* and
284 *GmMYBA1* identified 72 and 81 differential metabolites, respectively, whereas
285 *GmMYBA5* overexpression resulted in 37 differential metabolites (Fig. 6B). Among
286 these differential metabolites, 22, 52, and 64 were upregulated, while 15, 20 and 17
287 were down-regulated when comparing the overexpression of *GmMYBA5*, *GmMYBA2*
288 and *GmMYBA1*, respectively, with the empty vector (Fig. 6B, Supplementary Fig.
289 S7A-F). Notably, the numbers of up-regulated flavonoids metabolites were greater
290 than the number of down-regulated metabolites. Specially, out of the 37 differential
291 metabolites driven by the overexpression of *GmMYBA5*, 22 (59.5%) were
292 up-regulated, which is significantly lower than the numbers of the upregulated
293 metabolites driven by the overexpression of *GmMYBA2* (72.2%) and *GmMYBA1*
294 (79.0%) (Fig 6B). Among these up- and down-regulated metabolites, 20 (18.9%) were
295 shared by all of the three genes (Fig. 6C and Supplementary Table S2). Furthermore,
296 of the 72 differential metabolites driven by the overexpression of *GmMYBA2*, 61
297 (84.7%) were shared with *GmMYBA1*, suggesting potential redundancy in the

298 regulation of flavonoid synthesis between *GmMYBA2* and *GmMYBA1* (Fig. 6B and
299 C).

300 To further explore the regulatory role of these three *MYB* genes in anthocyanin
301 biosynthesis, we focused on the analysis of 12 anthocyanins. These 12 anthocyanins
302 encompassed cyanidin derivatives (idaein chloride, cyanin chloride, cyanidin
303 O-rutinoside, cyanidin 3-O-glucoside, keracyanin chloride), delphinidin derivatives
304 (myrtillin chloride, delphinidin chloride), pelargonidin derivatives (pelargonidin
305 chloride, callistephin chloride), and petunidin derivatives (petunidin 3-O-rutinoside,
306 petunidin 3-O-glucoside) (Fig. 6D). Our data showed that the majority of these 12
307 anthocyanins were upregulated in the overexpression lines of the three *MYB* genes.
308 Specially, in the *GmMYBA1* overexpression line, 10 (83.3%) out of the 12
309 anthocyanins were upregulated (Fig. 6D). In contrast, *GmMYBA5* overexpression
310 resulted in fewer and lower levels of anthocyanins in soybean hairy roots, which
311 could explain the reduced pigmentation observed in these roots. This observation is
312 consistent with the expression levels of catalytic enzymes genes (Fig. 6D). It is worth
313 noting that glycoside derivatives constituted a significant proportion (40.91% and
314 44.19%) of the differential metabolites between *GmMYBA5* and *GmMYBA2*, as well
315 as between *GmMYBA5* and *GmMYBA1* (Fig. 6D and Supplementary Table S3). These
316 data suggest that *GmMYBA5* has partially lost its function in regulating the expression
317 of genes involved in anthocyanin biosynthesis, resulting in reduced production of
318 glycoside derivatives. On the other hand, *GmMYBA2* and *GmMYBA1* appear to have
319 redundant functions in regulating the synthesis of flavonoids compounds including
320 anthocyanins.

321 **Discussion**

322 **MYB transcription factors are possible hotspots for tandem duplication**

323 Tandem duplication represents one of the key processes by which the copy number of
324 genes can be increased, leading to the emergence of new genetic resources during the
325 course of evolutionary history in many organisms. Certain classes, such as *R* genes,
326 are known to be prone to tandem duplication (Meyers et al., 2003; Innes et al., 2008).

327 It appears that *MYB* genes are also hotspots for tandem duplication in soybean, as well
328 as in several other species (O'Neil et al., 2007; Wang et al., 2023). Previous studies
329 have demonstrated that selection is relaxed on tandemly duplicated genes relative to
330 non-tandemly duplicated genes. This relaxed selection may allow more transposon
331 insertions or less efficient purging of transposons near these genes (Zhao et al., 2017).
332 However, this does not seem to be the case for the three *MYB* genes examined in our
333 study. Although these *MYB* genes have undergone functional divergence, they still
334 retain the function of the ancestral gene in regulating anthocyanin biosynthesis.
335 According to the gene dosage balance hypothesis, genes encoding proteins that
336 interact with other proteins are more sensitive to changes in order to maintain the
337 overall network functionality (Birchler and Veitia, 2021). Given that these *MYB* genes
338 function as transcription factors, they likely interact with other proteins, which could
339 explain their conserved function. Nevertheless, our study reveals a tissue-specific
340 pattern for these gene (Fig. 4A), a characteristic commonly observed in many other
341 tandemly duplicated genes (Zhao et al., 2017).

342 To understand the mechanism underlying *MYB* tandem duplication, we also
343 examined the transposon sequences within the genic and flanking regions of the three
344 *MYB* genes. Surprisingly, we found very few transposon sequences enriched in these
345 regions. However, considering the high rate of transposon turnover in soybean, it is
346 likely that the elements that contribute to the tandem duplication of the *MYB* genes
347 have already been eliminated from the genome. Further investigation could involve
348 examining other recently tandemly duplicated *MYB* gene clusters to assess the role of
349 transposons in mediating the tandem duplication of *MYB* genes.

350 **Functional divergence of the *MYB* duplicated genes**

351 Subfunctionalization proposes that duplicated genes originating from a common
352 ancestor specialize in complementary functions to maintain the original function of
353 their ancestral gene (Sandve et al., 2018). In our research, the tandemly duplicated
354 *MYB* genes have undergone both pseudogenization and subfunctionalization. A
355 putative pseudogene (*Glyma.09g235000*) structurally resembled the gene but lacked
356 expression and function. Other genes within the *MYB* gene cluster acted as activators

357 of anthocyanin synthesis but exhibited specialization in tissue-specific expression
358 patterns, varied activation abilities, and diverse downstream metabolites (Fig. 7).
359 Conserved MYB transcription factors contain activation domain in the C-terminal and
360 A binding domain in the N-terminal, enabling them to regulate anthocyanins synthesis
361 by forming MYB-bHLH-WD ternary complexes. (Wang et al., 2021). We have
362 demonstrated that variations in the BD contribute to the divergent anthocyanin
363 productions. The conserved bHLH-interacting motif [D/E]Lx2[R/ K]x3Lx6Lx3R is
364 present in GmMYBA5, GmMYBA2 and GmMYBA1, albeit with two substitutions of
365 L (Leucine) to M (Methionine) (Liu et al., 2015) (Supplementary Fig. S3). However,
366 whether these three genes exhibit distinct interaction preferences for basic
367 helix-loop-helix proteins, thereby resulting in the different metabolites, remains to be
368 determined.

369 *GmMYBA2* plays a regulatory role in the late stage of anthocyanin biosynthesis by
370 controlling enzymes such as flavonoid 3'5'hydroxylase, dihydroflavonol 4-reductase,
371 anthocyanidin synthase and glucosyltransferase, which are involved (Gao et al., 2021).
372 In contrast, overexpression of *GmMYBA5* led to reduced anthocyanin production,
373 indicating a partial loss of its regulatory function in regulating catalytic enzymes
374 genes. On the other hand, *GmMYBA2* and *GmMYBA1* exhibit functional redundancy
375 in regulating anthocyanidin synthesis, although they display distinct expression
376 patterns (Fig. 3A). Furthermore, the expression of *GmMYBA5* and *GmMYBA1* is
377 generally induced by abiotic and biotic stresses, as inferred from publicly available
378 RNA-seq libraries (<http://ipf.sustech.edu.cn/pub/soybean/>), suggesting their putative
379 function in adapting to changing environment factors (Zhang et al., 2020)
380 (Supplementary Fig. S8A-C). These results offer additional insights into the
381 evolutionary trajectory and function divergence resulting from gene duplication in the
382 regulation of plant secondary metabolites.

383 **Insights into the relationship of gene duplication and environmental adaptation**

384 Gene duplication is an important force for genome evolution and environmental
385 adaptation (Magadum et al., 2013; Chen et al., 2022b). Numerous studies have
386 highlighted the occurrence of adaptive gene duplications in response to environmental

387 stresses (Brown et al., 1998; Riehle et al., 2001; Hastings, 2007; James et al., 2008).
388 In our investigation of the collinear regions of the MYB transcription factors cluster
389 in legumes, we found that these orthologous *MYB* genes contribute to seed coat color
390 in common bean and cowpea (García-Fernández et al., 2021; Herniter et al., 2018).
391 The conservation of MYB transcription factors across species suggests their essential
392 role in enabling efficient responses to environmental stresses (Saigo et al., 2020). The
393 observed copy-number variation and functional divergence of *MYB* genes in legumes
394 serve as a compelling example of adaptive gene duplications in the evolutionary
395 history of legumes, which enhances our understanding of the role of gene duplications
396 as a mechanism of adaptation.

397 **Anthocyanin can be used as a morphological marker**

398 As Anthocyanin pigmentation can be identified by naked eyes, it has been employed
399 as a visible marker in the maize haploid inducer system, facilitating the efficient
400 selection of haploid embryos (Chen et al., 2022a). Selecting transgenic tissues and
401 plants during plant genetic transformation is a laborious and time-consuming process.
402 Recently, R2R3 type MYB transcription factors have been utilized as visible markers
403 for the selection of transformed tissues and plants in various species (Zhang et al.,
404 2019; Huang et al., 2021; Lim et al., 2022). Soybean hairy roots can be obtained by
405 *Agrobacterium rhizogenes* mediated transformation, forming chimera plants with
406 transformed hairy roots and untransformed shoots. In our study, we constructed plant
407 expression vectors containing the GmScreamM4 promoter (pM4), which drove the
408 expression of *GmMYBA2* and *GmMYBA1* in transgenic soybean hairy roots, leading to
409 the manifestation of a purple color (Fig. 5C). The application of *GmMYBA2* and
410 *GmMYBA1* as strong activators of anthocyanin biosynthesis in soybean holds
411 promising prospects for their utilization as markers to facilitate the effective
412 identification of transformed hairy roots.

413 **Materials and Methods**

414 **Plant materials**

415 The soybean cultivar Wm82 (Williams 82) was grown in the greenhouse at China

416 Agriculture University. Plant tissues were collected at the reproductive growth stage
417 R4 (full pod) and immediately frozen into liquid nitrogen before being stored at
418 -80 °C. The *Arabidopsis thaliana* ecotype Columbia was used for genetic
419 transformation. The transient ectopic expression material, tobacco (*Nicotiana*
420 *benthamiana*), was grown in the incubator with the constant temperature of 25°C.

421 **Estimation of evolutionary distance and analysis of micro-synteny**

422 To estimate evolutionary distance, we followed the method previously described
423 (Zhao et al. 2017; Yin et al. 2022). In brief, the coding sequences of the homologous
424 genes were aligned using ClustalW (Thompson et al., 1994) with default parameters,
425 followed by manual inspection. Pairwise alignments of the homologous genes were
426 performed to calculate Ka and Ks using the yn00 module under the PAML software
427 (Yang, 2007). Micro-synteny analysis was conducted using the LegumeInfo database
428 (<https://www.legumeinfo.org/>). The divergence time was obtained from the TimeTree
429 database (<https://timetree.org/>).

430 **cDNA synthesis and quantitative real-time PCR analysis**

431 Total RNA was isolated from soybean leaves, pods, stems and seeds by the StarSpin
432 HiPure Plant RNA Mini Kit (GenStar). To eliminate any genomic DNA contamination,
433 the StarScriptII First-strand cDNA Synthesis Mix With gDNA Remover (GenStar)
434 was employed to synthesize the first-strand complementary DNA (cDNA), following
435 the manufacturer's instructions. Quantitative real-time PCR (qRT-PCR) analysis was
436 performed using 2×RealStar Green Fast Mixture (with ROX II) (GenStar) according
437 to the manufacturer's protocol, and amplification was carried out using the ABI 7500
438 Real-time PCR system (Applied Biosystems, USA). The *Actin11* gene was used as the
439 internal control. The qRT-PCR data were analysed using the $2^{-\Delta\Delta Ct}$ analysis method.
440 Details of all the primers can be found in Supplementary Table S4.

441 **Analyses of phylogenetic relationship**

442 Sequence alignment of *GmMYBA5*, *GmMYBA2* and *GmMYBA1* was performed by
443 DNAMAN software version 8.0. A phylogenetic tree was constructed using the
444 Neighbor-Joining method in the MEGA7 program. The statistical significance of
445 individual nodes was assessed by bootstrap analysis with 1,000 replicates.

446 ***Arabidopsis thaliana* transformation**

447 The full-length coding sequences of *GmMYBA5*, *GmMYBA2* and *GmMYBA1* cloned
448 from Wm82 and the synthesized code sequence of *Glyma.09g235000* were introduced
449 into the pTF101 vector. The coding sequences were driven by the 35S promoter of
450 cauliflower mosaic virus (CaMV). The resulting constructs were then introduced into
451 *Agrobacterium* strain GV3101 for transformation of *Arabidopsis thaliana* using the
452 floral dip method (Bent, 2006). The presence of the constructs in the transgenic plants
453 was confirmed by PCR, followed by the sequencing of the PCR fragment with
454 specific primers. All primers used are listed in Supplementary Table S4.

455 **Subcellular localization**

456 The full-length CDS of *GmMYBA5*, *GmMYBA2* and *GmMYBA1* were cloned from
457 Wm82. These CDS sequences were fused in-frame with the GFP coding sequence and
458 subsequently inserted into a vector through combinational joining. The resulting
459 constructs were introduced into *Agrobacterium* strain GV3101 for infection of
460 *Nicotiana benthamiana* leaves. The GFP fluorescent signals emitted by the tobacco
461 leaf tissues were captured using a Zeiss confocal laser scanning microscope (Zeiss,
462 Germany).

463 **Transcriptional activation activity assay**

464 The transactivation activity assay was performed as previously described (Hou et al.,
465 2022). In brief, the coding sequences of *GmMYBA5*, *GmMYBA2* and *GmMYBA1* were
466 fused with the GAL4 DNA-binding domain (BD) in the plasmid pGBKT7. These
467 constructs were subsequently transformed into the yeast strain AH109 according to
468 the procedure previously described (Gietz et al., 2007). The yeast colonies were then
469 patched onto SD/-Trp and SD/-Trp/-His/-Ade plates and incubated at 30°C for 3 days.

470 **Transient ectopic expression in *Nicotiana benthamiana***

471 The pTF-gene constructs were used to perform transient ectopic expression in
472 *Nicotiana benthamiana*, following the procedure described earlier in the subcellular
473 localization section. After a 5-day incubation period, the phenotype of the infiltrated
474 leaf materials was observed, and the extracted anthocyanins were measured.

475 **Soybean hairy root transformation**

476 The 35S promoter of cauliflower mosaic virus (CaMV) in the plant expression vector
477 pTF101 was substituted with the pM4 promoter of soybean. The plasmids were then
478 transformed into *Agrobacterium rhizogenes* K599 for infection of soybean cotyledons
479 to generate transgenic soybean hairy roots. The procedure for transformation and
480 infection followed the method previously described with slight modifications (Kereszt
481 et al., 2007; Guo et al., 2011).

482 **Anthocyanin extractions and measurements**

483 Total anthocyanin contents were determined as previously described (Huang et al.,
484 2018). Plant tissues were collected and subsequently ground into powders using liquid
485 nitrogen. A total of 0.2 g powders was extracted in 1 ml of methanol containing 0.1%
486 (v/v) HCl, followed by incubation on ice for 30 min. After centrifugation at
487 12,000 rpm for 10 min, the supernatant was measured at 530 nm (A530) and 657 nm
488 (A657) using a spectrophotometer (SOPTOP, China). The relative content of
489 anthocyanin was calculated using the formula (A530-0.25×A657)/fresh weight.

490 **Metabolomics analysis**

491 Samples were prepared and metabolites were extracted following the protocols
492 provided by Novogene Co., Ltd. (Beijing, China). The extraction solution was then
493 injected into the LC-MS/MS system. LC-MS/MS analyses were performed using an
494 ExionLC™ AD system (SCIEX) coupled with a QTRAP® 6500+ mass spectrometer
495 (SCIEX) at Novogene Co., Ltd. (Beijing, China). The detection of the experimental
496 samples using Multiple Reaction Monitoring (MRM) was based on the in-house
497 database of Novogene. The generated data files from the HPLC-MS/MS were
498 processed using the SCIEX OS Version 1.4 to integrate and correct the peaks. Sample
499 normalization and significantly differential accumulated flavonoids were analyzed
500 using MetaboAnalyst 5.0 (<https://www.metaboanalyst.ca/>). Samples were normalized
501 by sum and the data were transformed using log10. The standard threshold criteria
502 were set as follows: $p \leq 0.05$ (Student's t test) and $|\log_2 FC| \geq 1$. Principal component
503 analysis (PCA) and hierarchical clustering were carried out using MetaboAnalyst 5.0
504 (<https://www.metaboanalyst.ca/>).

505

506 **Funding**

507 This work was supported by the National Natural Science Foundation of China (grant
508 nos. 32072089 and 31871708), the Recruitment Program of Global Experts and the
509 Fundamental Research Funds for the Central Universities (2022TC021).

510

511 **Author Contributions**

512 L.S. and M.Z. conceived and designed the project. R.M., Q.H., G.T. and J.L.
513 performed the experiments and W.H., J.A., T.F., and J.H. analysed the data. R.M.
514 wrote the manuscript. M.Z. and L.S. revised the paper. All authors read and approved
515 of this manuscript.

516

517 **Conflicts of Interest**

518 The authors declare that they have no conflicts of interest associated with this work.

519

520 **References**

521 **Albert NW, Davies KM, Lewis DH, Zhang H, Montefiori M, Brendolise C, Boase
522 MR, Ngo H, Jameson PE, Schwinn KE.** A conserved network of transcriptional
523 activators and repressors regulates anthocyanin pigmentation in eudicots. *Plant Cell*.
524 2014;**26**(3):962-980. <https://doi.org/10.1105/tpc.113.122069>

525 **Bent A.** *Arabidopsis thaliana* floral dip transformation method. *Methods Mol Biol*,
526 2006;**343**:87-103. <https://doi.org/10.1385/1-59745-130-4:87>

527 **Birchler JA, Veitia RA.** One hundred years of gene balance: how stoichiometric
528 issues affect gene expression, genome evolution, and quantitative traits. *Cytogenet
529 Genome Res*, 2021;**161**(10-11):529-550. <https://doi.org/10.1159/000519592>

530 **Brown CJ, Todd KM, Rosenzweig RF.** Multiple duplications of yeast hexose
531 transport genes in response to selection in a glucose-limited environment. *Mol Biol
532 Evol*, 1998;**15**(8):931-942. <https://doi.org/10.1093/oxfordjournals.molbev.a026009>

533 **Chen C, Liu XQ, Li SZ, Liu CX, Zhang YL, Luo LL, Miao LQ, Yang WZ, Xiao**

534 **ZJ, Zhong Y, et al.** Co-expression of transcription factors *ZmC1* and *ZmR2*
535 establishes an efficient and accurate haploid embryo identification system in maize.
536 *Plant J*, 2022a:111(5):1296-1307. <https://doi.org/10.1111/tpj.15888>

537 **Chen Y, Fang T, Su H, Duan SF, Ma RR, Wang P, Wu L, Sun WB, Hu QC, Zhao MX, et al.** A reference-grade genome assembly for *Astragalus mongholicus*
538 and insights into the biosynthesis and high accumulation of triterpenoids and
539 flavonoids in its roots. *Plant Commun*, 2022b:4:100469.
540 <https://doi.org/10.1016/j.xplc.2022.100469>

541 **Chin HS, Wu YP, Hour AL, Hong CY, Lin YR.** Genetic and evolutionary analysis
542 of purple leaf sheath in rice. *Rice*, 2016:9:8.
543 <https://doi.org/10.1186/s12284-016-0080-y>

544 **D'Amelia V, Aversano R, Ruggiero A, Batelli G, Appelhagen I, Dinacci C, Hill L, Martin C, Carputo D.** Subfunctionalization of duplicate MYB genes in *Solanum commersonii* generated the cold-induced *ScAN2* and the anthocyanin regulator *ScAN1*.
545 *Plant Cell and Environ*, 2018: 41(5):1038-1051. <https://doi.org/10.1111/pce.12966>

546 **Freeling M.** Bias in plant gene content following different sorts of duplication:
547 tandem, whole-genome, segmental, or by transposition. *Annu Rev of Plant Biol*,
548 2009:60:433-453. <https://doi.org/10.1146/annurev.arplant.043008.092122>

549 **Gao RF, Han TT, Xun HW, Zeng XS, Li PH, Li YQ, Wang YN, Shao Y, Cheng X, Feng XZ, et al.** MYB transcription factors *GmMYBA2* and *GmMYBR* function in a
550 feedback loop to control pigmentation of seed coat in soybean. *J Exp Bot*,
551 2021:72(12):4401-4418. <https://doi.org/10.1093/jxb/erab152>

552 **García-Fernández C, Campa A, Ferreira JJ.** Dissecting the genetic control of seed
553 coat color in a RIL population of common bean (*Phaseolus vulgaris* L.). *Theor and
554 Appl Genet*, 2021:134(11):3687-3698. <https://doi.org/10.1007/s00122-021-03922-y>

555 **Gietz RD, Schiestl RH.** High-efficiency yeast transformation using the LiAc/SS
556 carrier DNA/PEG method. *Nat Protoc*, 2007:2(1):31-34.
557 <https://doi.org/10.1038/nprot.2007.13>

558 **Gillman JD, Tetlow A, Lee JD, Shannon JG, Bilyeu K.** Loss-of-function mutations
559 affecting a specific *Glycine max* R2R3 MYB transcription factor result in brown
560 *Plant J*, 2022a:111(5):1296-1307. <https://doi.org/10.1111/tpj.15888>

561 <https://doi.org/10.1016/j.xplc.2022.100469>

562 **Gillman JD, Tetlow A, Lee JD, Shannon JG, Bilyeu K.** Loss-of-function mutations
563 affecting a specific *Glycine max* R2R3 MYB transcription factor result in brown

564 hilum and brown seed coats. *BMC Plant Biol*, 2011;**11**:155 <https://doi.org/10.1186/1471-2229-11-155>

565

566 **Gould KS.** Nature's Swiss Army Knife: The diverse protective roles of anthocyanins

567 in leaves. *J of Biomed and Biotechnol*, 2004;**2004**(5):314-320.

568 <https://doi.org/10.1155/S1110724304406147>

569 **Grotewold E, Drummond BJ, Bowen B, Peterson T.** The MYB-homologous

570 *p-gene* controls phlobaphene pigmentation in maize floral organs by directly

571 activating a flavonoid biosynthetic gene subset. *Cell*, 1994;**76**(3):543-553.

572 [https://doi.org/10.1016/0092-8674\(94\)90117-1](https://doi.org/10.1016/0092-8674(94)90117-1)

573 **Guo WB, Zhao J, Li XX, Qin L, Yan XL, Liao H.** A soybean β -expansin gene

574 *GmEXPB2* intrinsically involved in root system architecture responses to abiotic

575 stresses. *Plant J*, 2011;**66**(3):541-552.

576 <https://doi.org/10.1111/j.1365-313X.2011.04511.x>

577 **Hastings PJ.** Adaptive amplification. *Crit Rev Biochem and Mol Biol*,

578 2007;**42**(4):271-283. <https://doi.org/10.1080/10409230701507757>

579 **Herniter IA, Muñoz-Amatriaín M, Lo S, Guo YN, Close TJ.** Identification of

580 candidate genes controlling black seed coat and pod tip color in cowpea (*Vigna*

581 *unguiculata* [L.] Walp). *G3* (Bethesda), 2018;**8**(10):3347-3355.

582 <https://doi.org/10.1534/g3.118.200521>

583 **Hichri I, Barrieu F, Bogs J, Kappel C, Delrot S, Lauvergeat V.** Recent advances in

584 the transcriptional regulation of the flavonoid biosynthetic pathway. *J Exp Bot*,

585 2011;**62**(8):2465-2483. <https://doi.org/10.1093/jxb/erq442>

586 **Hou JJ, Fan WW, Ma RR, Li B, Yuan ZH, Huang WX, Wu YY, Hu Q, Lin CJ,**

587 **Zhao XQ, et al.** *MALE STERILITY 3* encodes a plant homeodomain-finger protein for

588 male fertility in soybean. *J Integr Plant Biol*, 2022;**64**(5):1076-1086.

589 <https://doi.org/10.1111/jipb.13242>

590 **Huang D, Wang X, Tang ZZ, Yuan Y, Xu YT, He JX, Jiang XL, Peng SA, Li L,**

591 **Butelli E, et al.** Subfunctionalization of the *Ruby2-Ruby1* gene cluster during the

592 domestication of citrus. *Nat Plants*, 2018;**4**(11):930-941.

593 <https://doi.org/10.1038/s41477-018-0287-6>

594 **Huang T, Xin S, Fang Y, Chen T, Chang J, Ko N, Huang H, Hua Y.** Use of a
595 novel R2R3-MYB transcriptional activator of anthocyanin biosynthesis as visual
596 selection marker for rubber tree (*Hevea brasiliensis*) transformation. Ind Crop and
597 Prod, 2021;174:114225. <https://doi.org/10.1016/j.indcrop.2021.114225>

598 **Innes RW, Ameline-Torregrosa C, Ashfield T, Cannon E, Cannon SB, Chacko B, Chen NW, Couloux A, Dalwani A, Denny R, et al.** Differential accumulation of
599 retroelements and diversification of NB-LRR disease resistance genes in duplicated
600 regions following polyploidy in the ancestor of soybean. Plant Physiology, 2008;148(4):1740-1759. <https://doi.org/10.1104/pp.108.127902>

601 **James TC, Usher J, Campbell S, Bond U.** Lager yeasts possess dynamic genomes
602 that undergo rearrangements and gene amplification in response to stress. Curr Genet,
603 2008;53(3):139-152. <https://doi.org/10.1007/s00294-007-0172-8>

604 **Jeong SC, Moon JK, Park SK, Kim MS, Lee K, Lee SR, Jeong N, Choi MS, Kim N, Kang ST, et al.** Genetic diversity patterns and domestication origin of soybean.
605 Theor Appl Genet, 2019;132(4):1179-1193.
606 <https://doi.org/10.1007/s00122-018-3271-7>

607 **Kereszt A, Li D, Indrasumunar A, Nguyen CD, Nontachaiyapoom S, Kinkema M, Gresshoff PM.** *Agrobacterium rhizogenes*-mediated transformation of soybean to
608 study root biology. Nat Protoc, 2007;2(4):948-952.
609 <https://doi.org/10.1038/nprot.2007.141>

610 **Kim MY, Van K, Kang YJ, Kim KH, Lee SH.** Tracing soybean domestication
611 history: From nucleotide to genome. Breeding Sci, 2012;61(5):445-452.
612 <https://doi.org/10.1270/jsbbs.61.445>

613 **Kovinich N, Kayanja G, Chanoca A, Otegui MS, Grotewold E.** Abiotic stresses
614 induce different localizations of anthocyanins in *Arabidopsis*. Plant Signal Behav,
615 2015;10(7):1027850. <https://doi.org/10.1080/15592324.2015.1027850>

616 **Li CX, Yu WJ, Xu JR, Lu XF, Liu YZ.** Anthocyanin biosynthesis induced by MYB
617 transcription factors in plants. Int J Mol Sci, 2022a;23(19):11701.
618 <https://doi.org/10.3390/ijms231911701>

619 **Li Y, Fang XJ, Lin ZW.** Convergent loss of anthocyanin pigments is controlled by

624 the same MYB gene in cereals. *J Exp Bot*, 2022b:**73**(18):6089-6102.
625 <https://doi.org/10.1093/jxb/erac270>

626 **Li YH, Guan RX, Liu ZX, Ma YS, Wang LX, Li LH, Lin FY, Luan WJ, Chen**
627 **PY, Yan Z, et al.** Genetic structure and diversity of cultivated soybean (*Glycine max*
628 (L.) Merr.) landraces in China. *Theor Appl Genet*, 2008:**117**(6):857-871.
629 <https://doi.org/10.1007/s00122-008-0825-0>

630 **Lim SH, Kim DH, Cho MC, Lee JY.** Chili Pepper *AN2* (*CaAN2*): A visible
631 selection marker for nondestructive monitoring of transgenic plants. *Plants* (Basel),
632 2022.**11**(6):820. <https://doi.org/10.3390/plants11060820>

633 **Liu JY, Osbourn A, Ma PD.** MYB Transcription Factors as Regulators of
634 Phenylpropanoid Metabolism in Plants. *Mol Plant*, 2015:**8**(5):689-708.
635 <https://doi.org/10.1016/j.molp.2015.03.012>

636 **Lloyd A, Brockman A, Aguirre L, Campbell A, Bean A, Cantero A, Gonzalez A.**
637 Advances in the MYB-bHLH-WD Repeat (MBW) pigment regulatory model:
638 Addition of a WRKY factor and co-option of an anthocyanin MYB for betalain
639 regulation. *Plant and Cell Physiol*, 2017: **58**(9):1431-1441.
640 <https://doi.org/10.1093/pcp/pcx075>

641 **Lu N, Rao X, Li Y, Jun JH, Dixon RA.** Dissecting the transcriptional regulation of
642 proanthocyanidin and anthocyanin biosynthesis in soybean (*Glycine max*). *Plant*
643 *Biotechnol J*, 2021:**19**(7):1429-1442. <https://doi.org/10.1111/pbi.13562>

644 **Magadum S, Banerjee U, Murugan P, Gangapur D, Ravikesavan R.** Gene
645 duplication as a major force in evolution. *J Genet*, 2013:**92**(1):155-161.
646 <https://doi.org/10.1007/s12041-013-0212-8>

647 **Malle S, Morrison M, Belzile F.** Identification of loci controlling mineral element
648 concentration in soybean seeds. *BMC Plant Biol*, 2020:**20**(1):419.
649 <https://doi.org/10.1186/s12870-020-02631-w>

650 **Meyers BC, Kozik A, Griego A, Kuang H, Michelmore RW.** Genome-wide
651 analysis of NBS-LRR-encoding genes in *Arabidopsis*. *Plant Cell*, 2003:**15**(4):809-834.
652 <https://doi.org/10.1105/tpc.009308>

653 **O'Neil J, Tchinda J, Gutierrez A, Moreau L, Maser RS, Wong KK, Li W,**

654 **McKenna K, Liu XS, Feng B, et al.** Alu elements mediate MYB gene tandem
655 duplication in human T-ALL. *J Exp Med*, 2007;**204**(13):3059-3066.
656 <https://doi.org/10.1084/jem.20071637>

657 **Putta S, Yarla NS, Peluso I, Tiwari DK, Reddy GV, Giri PV, Kumar N, Malla R, Rachel V, Bramhachari PV, et al.** Anthocyanins: Multi-target agents for prevention
658 and therapy of chronic diseases. *Cur Pharm Des*, 2017;**23**(41):6321-6346.
660 <https://doi.org/10.2174/1381612823666170519151801>

661 **Riehle MM, Bennett AF, Long AD.** Genetic architecture of thermal adaptation in
662 *Escherichia coli*. *Proc Natl Acad Sci U S A*, 2001;**98**(2):525-530.
663 <https://doi.org/10.1073/pnas.98.2.525>

664 **Rizzon C, Ponger L, Gaut BS.** Striking similarities in the genomic distribution of
665 tandemly arrayed genes in *Arabidopsis* and rice. *PLoS Comput Biol*, 2006;**2**(9):115.
666 <https://doi.org/10.1371/journal.pcbi.0020115>

667 **Saigo T, Wang T, Watanabe M, Tohge T.** Diversity of anthocyanin and
668 proanthocyanin biosynthesis in land plants. *Curr Opin Plant Biol*, 2020;**55**:93-99.
669 <https://doi.org/10.1016/j.pbi.2020.04.001>

670 **Sandve SR, Rohlfs RV, Hvidsten TR.** Subfunctionalization versus
671 neofunctionalization after whole-genome duplication. *Nat Genet*, 2018;**50**(7):908-909.
672 <https://doi.org/10.1038/s41588-018-0162-4>

673 **Shin DH, Choi MG, Kang CS, Park CS, Choi SB, Park YI.** A wheat R2R3-MYB
674 protein *PURPLE PLANT1 (TaPL1)* functions as a positive regulator of anthocyanin
675 biosynthesis. *Biochem Biophys Res Commun*, 2016;**469**(3):686-691.
676 <https://doi.org/10.1016/j.bbrc.2015.12.001>

677 **Soltis PS, Marchant DB, Van de Peer Y, Soltis DE.** Polyploidy and genome
678 evolution in plants. *Curr Opin Genet Dev*, 2015;**35**:119-125.
679 <https://doi.org/10.1016/j.gde.2015.11.003>

680 **Soltis PS, Soltis DE.** Ancient WGD events as drivers of key innovations in
681 angiosperms. *Curr Opin Plant Biol*, 2016;**30**:159-165.
682 <https://doi.org/10.1016/j.pbi.2016.03.015>

683 **Stracke R, Werber M, Weisshaar B.** The R2R3-MYB gene family in *Arabidopsis*

684 *thaliana*. Curr Opin Plant Biol, 2001;4(5):447-456.
685 [https://doi.org/10.1016/s1369-5266\(00\)00199-0](https://doi.org/10.1016/s1369-5266(00)00199-0)

686 **Sundaramoorthy J, Park GT, Lee JD, Kim JH, Seo HS, Song JT.** Genetic and
687 molecular regulation of flower pigmentation in soybean. J KOREAN SOC APPL BI,
688 2015; 58(4):555-562. <https://doi.org/10.1007/s13765-015-0077-z>

689 **Thompson JD, Higgins DG, Gibson TJ.** CLUSTAL W: Improving the sensitivity of
690 progressive multiple sequence alignment through sequence weighting,
691 position-specific gap penalties and weight matrix choice. Nucleic Acids Res,
692 1994;22(22):4673-4680. <https://doi.org/10.1093/nar/22.22.4673>

693 **Wang CN, Ji WK, Liu YC, Zhou P, Meng YY, Zhang PC, Wen JQ, Mysore KS,**
694 **Zhai JX, Young ND, et al.** The antagonistic MYB paralogs *RH1* and *RH2* govern
695 anthocyanin leaf markings in *Medicago truncatula*. New Phytol,
696 2021;229(6):3330-3344. <https://doi.org/10.1111/nph.17097>

697 **Wang JP, Sun PC, Li YX, Liu YZ, Yu JG, Ma XL, Sun SR, Yang NS, Xia RY,**
698 **Lei TY, et al.** Hierarchically aligning 10 legume genomes establishes a family-level
699 genomics platform. Plant Physiol, 2017;174(1):284-300.
700 <https://doi.org/10.1104/pp.16.01981>.

701 **Wang S, Xu Z, Yang Y, Ren W, Fang J, Wan L.** Genome-wide analysis of
702 R2R3-MYB genes in cultivated peanut (*Arachis hypogaea* L.): Gene duplications,
703 functional conservation, and diversification. Front Plant Sci, 2023;14:1102174
704 <https://doi.org/1102174.10.3389/fpls.2023.1102174>

705 **Wang XP, Wang W, Chen SY, Lian YJ, Wang SC.** *Tropaeolum majus* R2R3 MYB
706 transcription factor *TmPAP2* functions as a positive regulator of anthocyanin
707 biosynthesis. Int J Mol Sci, 2022;23(20):12395.
708 <https://doi.org/10.3390/ijms232012395>

709 **Xie M, Chung CY, Li MW, Wong FL, Wang X, Liu A, Wang Z, Leung AK,**
710 **Wong TH, Tong SW, et al.** A reference-grade wild soybean genome. Nat Commun,
711 2019;10(1):1216. <https://doi.org/10.1038/s41467-019-09142-9>

712 **Xu WJ, Dubos C, Lepiniec, L.** Transcriptional control of flavonoid biosynthesis by
713 MYB-bHLH-WDR complexes. Trends in Plant Sci, 2015;20(3):176-185.

714 <https://doi.org/10.1016/j.tplants.2014.12.001>

715 **Yang ZH.** PAML 4: phylogenetic analysis by maximum likelihood. Mol Biol Evol, 716 2007;**24**(8):1586-1591. <https://doi.org/10.1093/molbev/msm088>

717 **Yin LW, Xu G, Yang JL, Zhao MX.** The heterogeneity in the landscape of gene 718 dominance in maize is accompanied by unique chromatin environments. Mol Biol 719 Evol, 2022;**39**(10). <https://doi.org/10.1093/molbev/msac198>

720 **Zabala G, Vodkin LO.** Methylation affects transposition and splicing of a large 721 CACTA transposon from a MYB transcription factor regulating anthocyanin synthase 722 genes in soybean seed coats. PLoS One, 2014;**9**(11):111959. 723 <https://doi.org/10.1371/journal.pone.0111959>

724 **Zhang H, Zhang F, Yu YM, Feng L, Jia JB, Liu B, Li BS, Guo HW, Zhai JX.** A 725 comprehensive online database for exploring ~20,000 public *Arabidopsis* RNA-seq 726 libraries. Mol Plant, 2020;**13**(9):1231-1233. 727 <https://doi.org/10.1016/j.molp.2020.08.001>

728 **Zhang N, McHale LK, Finer JJ.** Isolation and characterization of "GmScream" 729 promoters that regulate highly expressing soybean (*Glycine max*. Merr.) genes. Plant 730 Sci, 2015;**241**:189-198. <https://doi.org/10.1016/j.plantsci.2015.10.010>

731 **Zhang P, Chopra S, Peterson T.** A segmental gene duplication generated 732 differentially expressed myb-homologous genes in maize. Plant Cell, 733 2000;**12**(12):2311-2322. <https://doi.org/10.1105/tpc.12.12.2311>

734 **Zhang SL, Kondorosi É, Kereszt A.** An anthocyanin marker for direct visualization 735 of plant transformation and its use to study nitrogen-fixing nodule development. J 736 Plant Res, 2019;**132**(5):695-703. <https://doi.org/10.1007/s10265-019-01126-6>

737 **Zhang Y, Butelli E, Martin C.** Engineering anthocyanin biosynthesis in plants. Curr 738 Opin Plant Biol, 2014;**19**:81-90. <https://doi.org/10.1016/j.pbi.2014.05.011>

739 **Zhao MX, Zhang B, Lisch D, Ma JX.** Patterns and consequences of subgenome 740 differentiation provide insights into the nature of paleopolyploidy in plants. Plant Cell, 741 2017;**29**(12):2974-2994. <https://doi.org/10.1105/tpc.17.00595>

742

743 **Figure Legends**

744 **Figure 1. Micro-synteny analysis of the *MYB* gene cluster in legumes.**

745 (A) *GmMYBA5* (*Glyma.09g234900*), *GmMYBA2* (*Glyma.09g235100*), *GmMYBA1*
746 (*Glyma.09g235300*) and the pseudogene (*Glyma.09g235000*) are located in a cluster
747 on chromosome 9.

748 (B) Micro-synteny analysis of the *MYB* gene cluster in legumes. Each triangle
749 represents a gene and the tip of the triangle indicates the direction of the gene. Genes
750 belonging to the same family are depicted using the same color.

751

752 **Figure 2. *GmMYBA5*, *GmMYBA2* and *GmMYBA1* are closely clustered and**
753 **phylogenetically related in the soybean genome.**

754 (A) An amino acid sequence alignment of *GmMYBA5*, *GmMYBA2* and *GmMYBA1*.
755 The conserved KPRPR[S/T] [F/L] motif in subgroup 6 involved in anthocyanin
756 regulation (activation) is highlighted in a red box.

757 (B) Phylogenetic analysis of *MYB* genes involved in the anthocyanin and
758 proanthocyanin pathways. The protein sequences were used to construct the
759 phylogenetic tree using the neighbor-joining method in MEGA7, with 1000 bootstrap
760 replicates. The numbers displayed at each node represent the bootstrap values that
761 support the corresponding node, with values above 50% from 1000 replicates being
762 shown. The GenBank accession numbers corresponding to the *MYB* proteins are
763 listed in Table S5.

764

765 **Figure 3. *GmMYBA5*, *GmMYBA2* and *GmMYBA1* function as transcriptional**
766 **activators.**

767 (A) Subcellular localization of *GmMYBA5*, *GmMYBA2* and *GmMYBA1* in tobacco
768 (*Nicotiana benthamiana*) leaf epidermal cells. Bars = 25 μ m.

769 (B) Transactivation activity assays in yeast demonstrated strong transactivation
770 activity for *GmMYBA5*, *GmMYBA2* and *GmMYBA1*.

771 (C) Phenotype characteristics of *Arabidopsis* transgenic lines and wild type controls.

772 WT, wild type; A5, 35S:*GmMYBA5*; A2, 35S:*GmMYBA2*; A1, 35S:*GmMYBA1*. Bars
773 = 0.15 cm.

774

775 **Figure 4. Functional divergence of the duplicated *MYB* genes.**

776 (A) Gene expression analysis of *GmMYBA5*, *GmMYBA2* and *GmMYBA1* in different
777 tissues of soybean.

778 (B) *Nicotiana benthamiana* leaves and total anthocyanin after the transient
779 overexpression of *GmMYBA5*, *GmMYBA2*, *GmMYBA1* and the control with an empty
780 vector (EV). Bar = 1 cm.

781 (C) Overexpression of *GmMYBA5*, *GmMYBA2* and *GmMYBA1* induced significant
782 enrichment of anthocyanins. The relative anthocyanin contents were quantified using
783 the formula $(A530-0.25 \times A657)/\text{fresh weight}$, representing one anthocyanin unit. The
784 data indicates the mean \pm SD for three biological replicates. Statistical significance
785 was determined using Student's *t* test (***, $p < 0.001$).

786

787 **Figure 5. Molecular basis underlying the functional divergence of the *MYB*
788 genes.**

789 (A) Chimeric proteins generated by fusing the DNA binding domains (BD) and
790 activating domains (AD) from *GmMYBA5*, *GmMYBA2*, and *GmMYBA1*.

791 (B) *Nicotiana benthamiana* leaves and total anthocyanin after the transient expression
792 of different chimeric proteins. Bar = 1 cm.

793 (C) Transgenic soybean hairy roots of Wm82 overexpressing empty vector (EV) and
794 *GmMYBA5*, *GmMYBA2* and *GmMYBA1* with pM4. Bar = 0.25 cm.

795 (D) Expression analyses of anthocyanin-related genes in transgenic soybean hairy
796 roots of Wm82 overexpressing empty vector (EV) and *GmMYBA5*, *GmMYBA2* and
797 *GmMYBA1* with pM4. Different lowercase letters indicate significant differences
798 among groups based on Fisher's Least Significant Difference (LSD) test at $P < 0.05$.

799

800 **Figure 6. Metabolomics analysis of soybean hairy roots overexpressing the *MYB*
801 genes revealed distinct types and abundances of downstream metabolites.**

802 (A) Classification and number of all flavonoids detected across the samples.
803 (B) Number of differential metabolites between all comparisons. The numbers of
804 up-regulated metabolites and down-regulated metabolites are shown in the histogram.
805 EV, empty vector; A5, pM4:*GmMYBA5*; A2, pM4:*GmMYBA2*; A1, pM4:*GmMYBA1*.
806 (C) Venn analysis depicting the overlapping and unique differential metabolites in
807 hairy roots overexpressing *GmMYBA5*, *GmMYBA2* and *GmMYBA1*. A5,
808 pM4:*GmMYBA5*; A2, pM4:*GmMYBA2*; A1, pM4:*GmMYBA1*.
809 (D) Types and changes of anthocyanins detected in the overexpression lines of
810 *GmMYBA5*, *GmMYBA2*, and *GmMYBA1*. Glycoside derivatives are highlighted in
811 red.
812

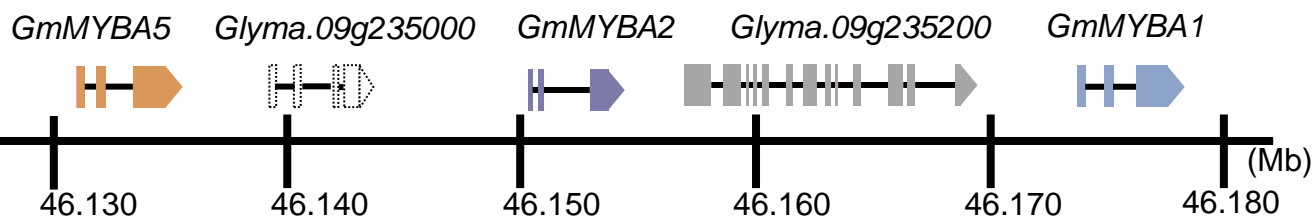
813 **Figure 7. The model of the tandemly duplicated *MYB* genes functionally diverged**
814 **in the regulation of anthocyanin biosynthesis pathway.**

815 The *MYB* genes following tandem duplication undergone functional divergence,
816 leading to tissue-specific expression patterns and differential activation abilities for
817 anthocyanin biosynthesis pathway. CHI, chalcone isomerase; DFR,
818 dihydroflavonol-4-reductase; F3'H, flavonoid 3'-hydroxylase; F3'5'H, flavonoid
819 3'5'hydroxylase; F3H, flavanone 3-hydroxylase; DFR, Dihydroflavonol 4-reductase;
820 ANS, anthocyanidin synthase; UFGT, UDP-flavonoid glucosyltransferase.

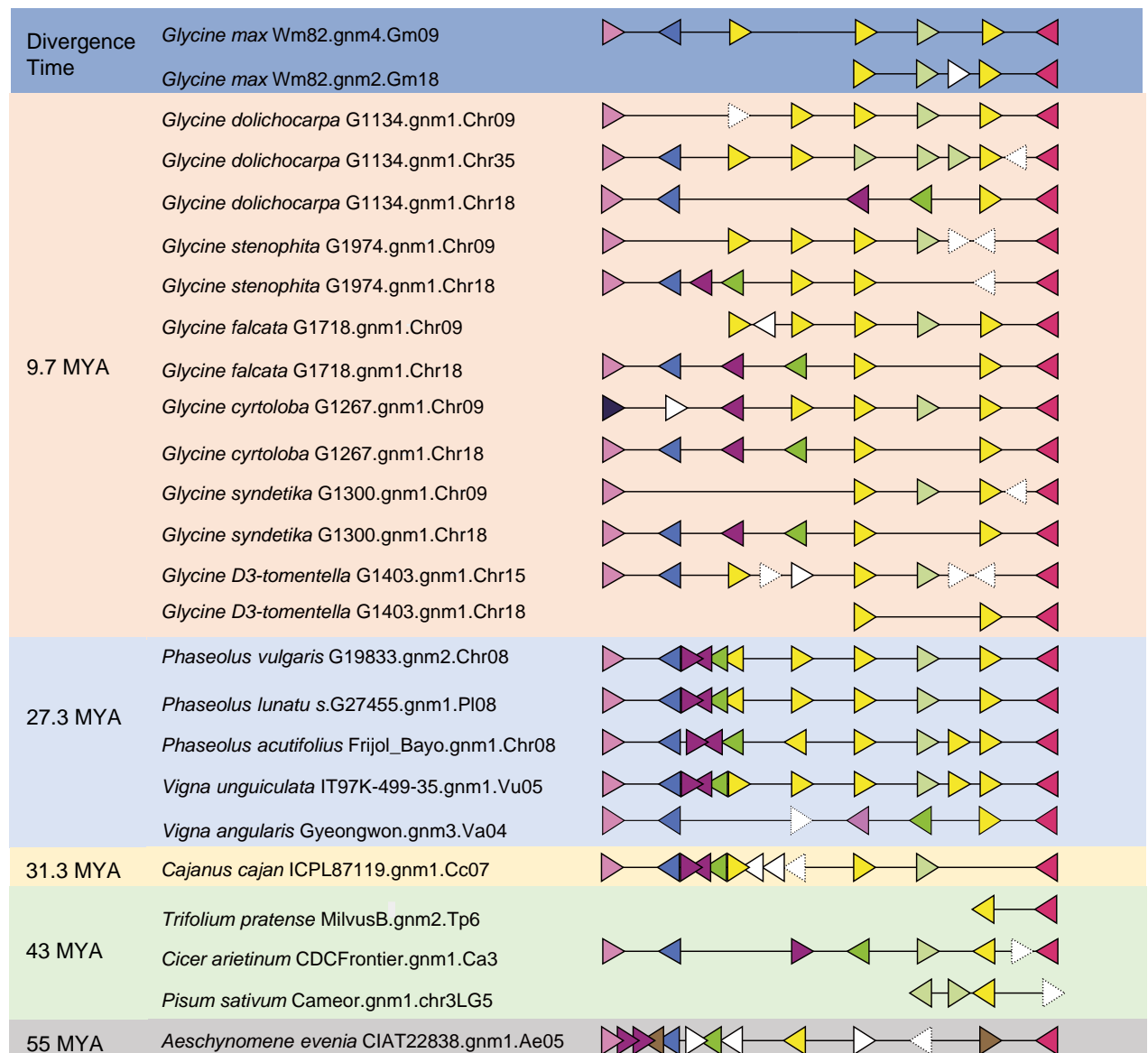
Table 1. Evolutionary distances of the three MYB genes within soybean and between soybean and common bean

MYB gene	Homologous gene in soybean or common bean	Ka	Ks	ω (Ka/Ks)
<i>Glyma.09G234900 (GmMYBA5)</i>	<i>Phvul.008G038200</i>	0.1823	0.3714	0.4907
<i>Glyma.09G235100 (GmMYBA2)</i>	<i>Phvul.008G038200</i>	0.1776	0.3972	0.4471
<i>Glyma.09G235300 (GmMYBA1)</i>	<i>Phvul.008G038200</i>	0.1843	0.4659	0.3956
<i>Glyma.09G234900 (GmMYBA5)</i>	<i>Glyma.09G235100 (GmMYBA2)</i>	0.0758	0.2030	0.3735
<i>Glyma.09G234900 (GmMYBA5)</i>	<i>Glyma.09G235300 (GmMYBA1)</i>	0.0940	0.2758	0.3407
<i>Glyma.09G235100 (GmMYBA2)</i>	<i>Glyma.09G235300 (GmMYBA1)</i>	0.0880	0.2721	0.3234
<i>Phvul.008G038200</i>	<i>Phvul.008G038400</i>	0.1740	0.4100	0.4244
<i>Phvul.008G038200</i>	<i>Phvul.008G038500</i>	0.2020	0.6456	0.3128
<i>Phvul.008G038200</i>	<i>Phvul.008G038600</i>	0.0356	0.0654	0.5444
<i>Phvul.008G038400</i>	<i>Phvul.008G038500</i>	0.0821	0.1414	0.5810
<i>Phvul.008G038400</i>	<i>Phvul.008G038600</i>	0.1904	0.5139	0.3705
<i>Phvul.008G038500</i>	<i>Phvul.008G038600</i>	0.2131	0.6243	0.3413

A

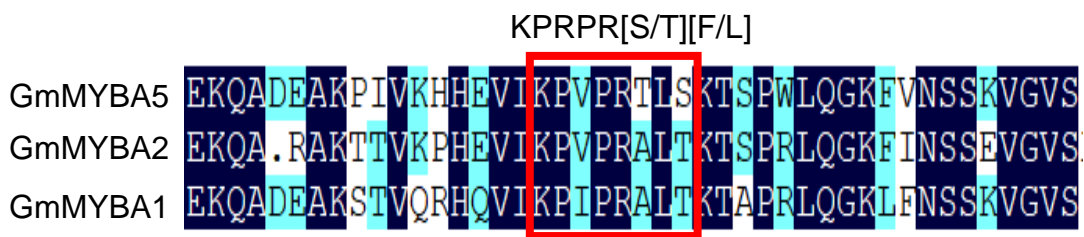


B

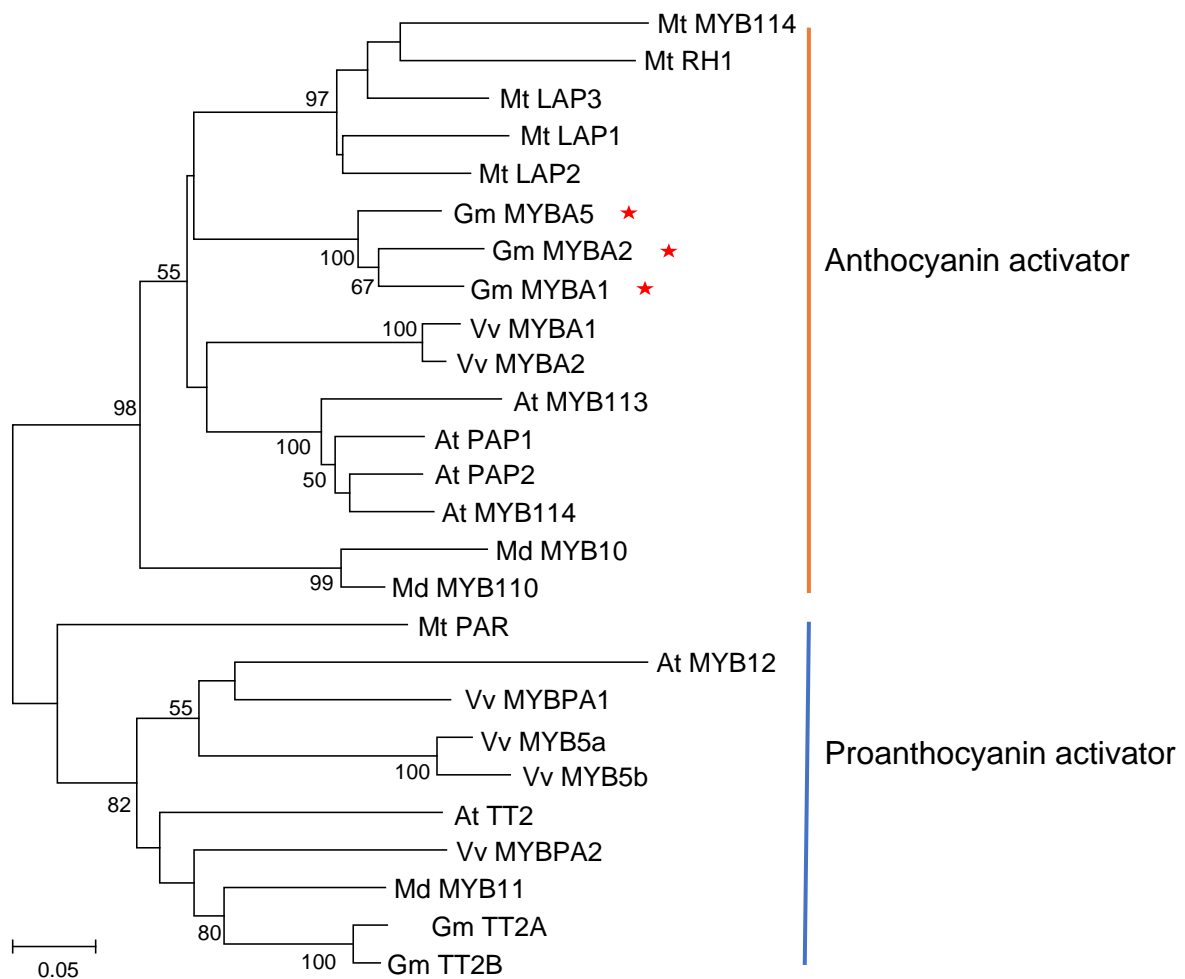


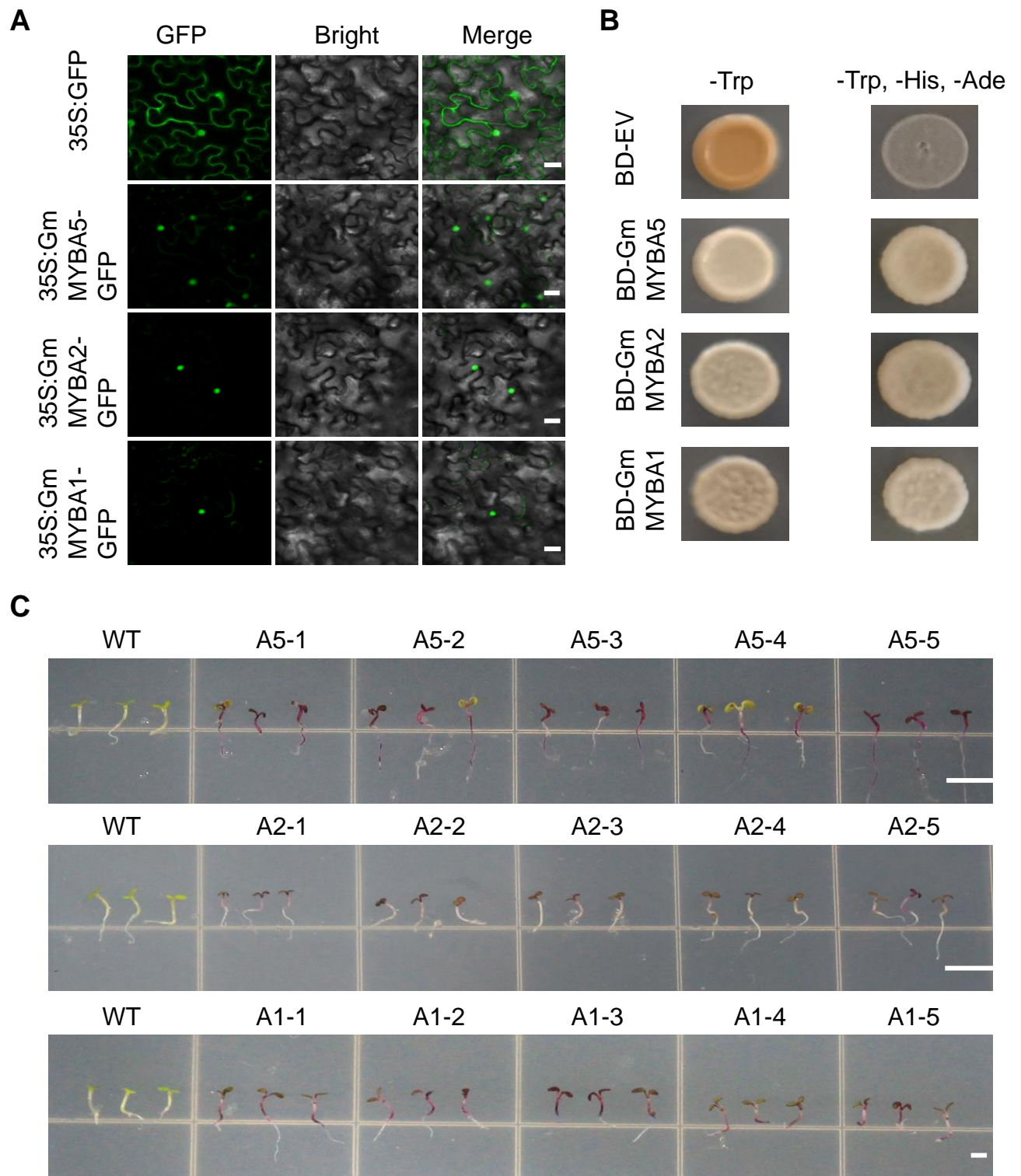
- ▶ MYB transcription factor
- ▶ Vesicle transport v-SNARE family protein
- ▶ Singletons
- ▶ Phosphate transporter PHO1 homolog
- ▶ Cystathionine Gamma-Synthase
- ▶ Orphans
- ▶ Pentatricopeptide repeat (PPR) superfamily protein
- ▶ emp24/gp25L/p24 family/GOLD family protein
- ▶ Pectinesterase
- ▶ Protein of unknown function

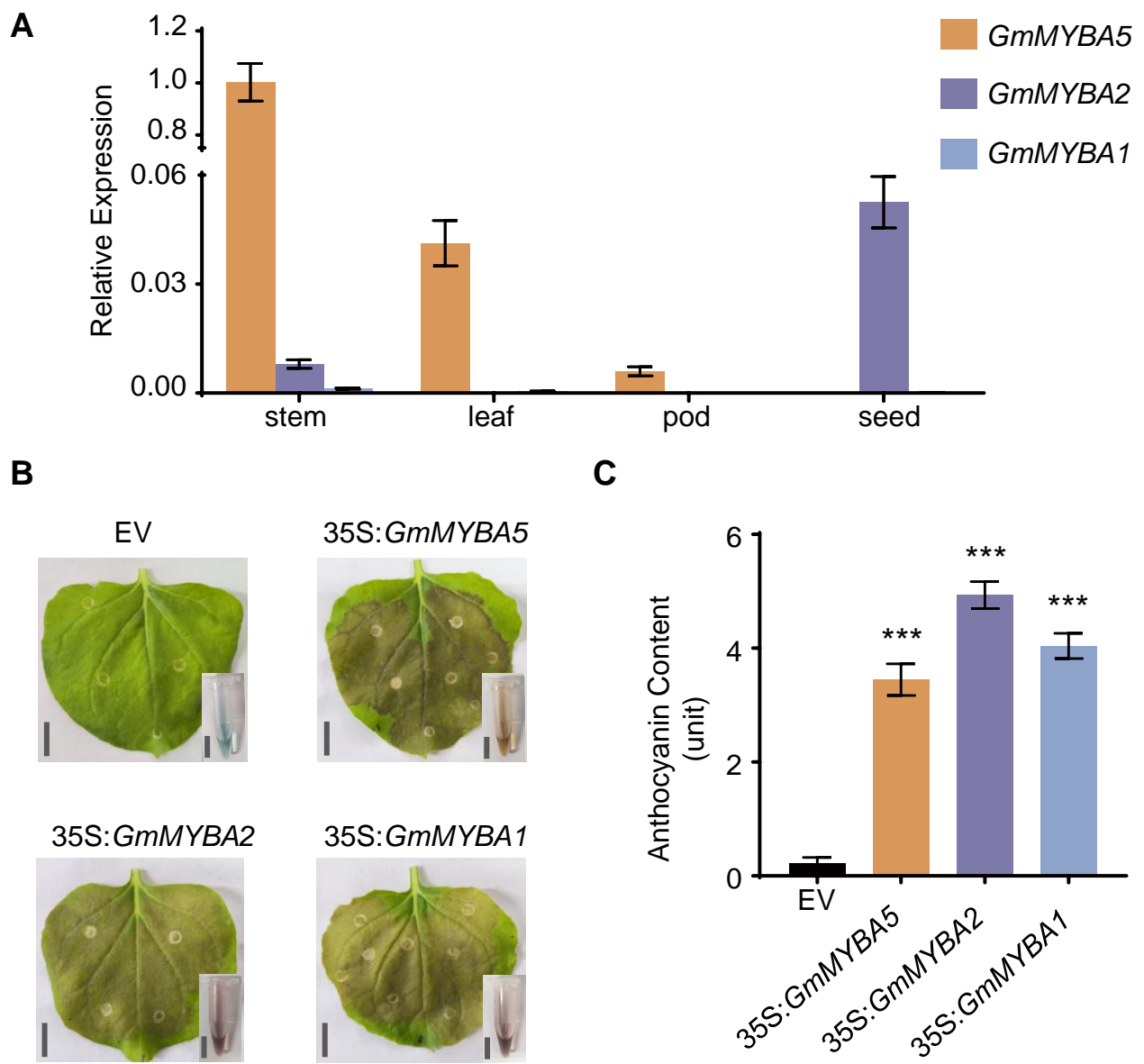
A



B



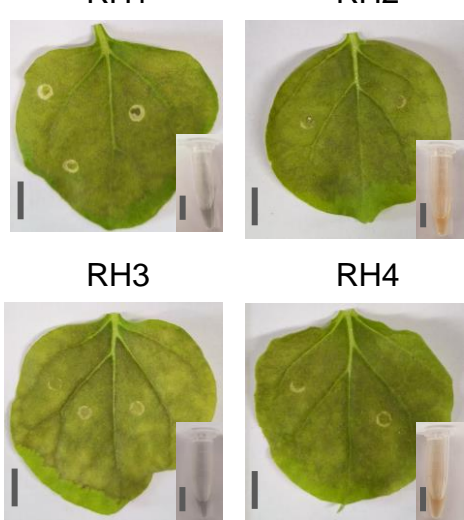




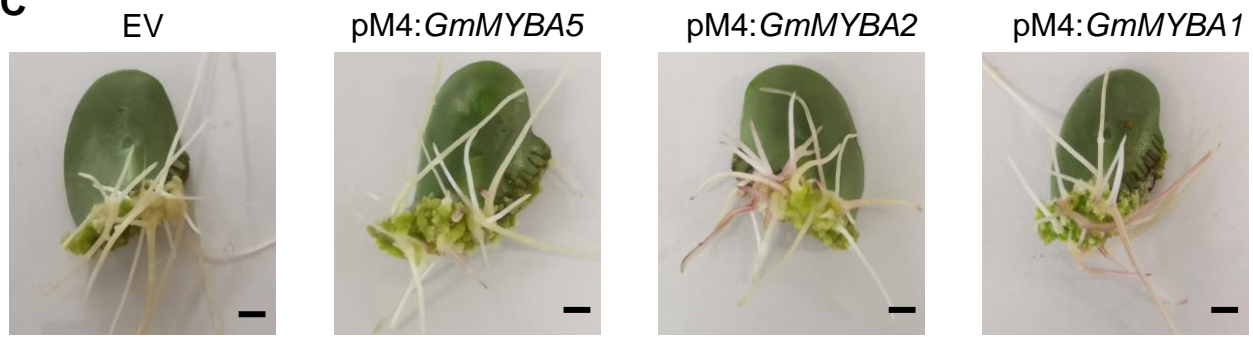
A



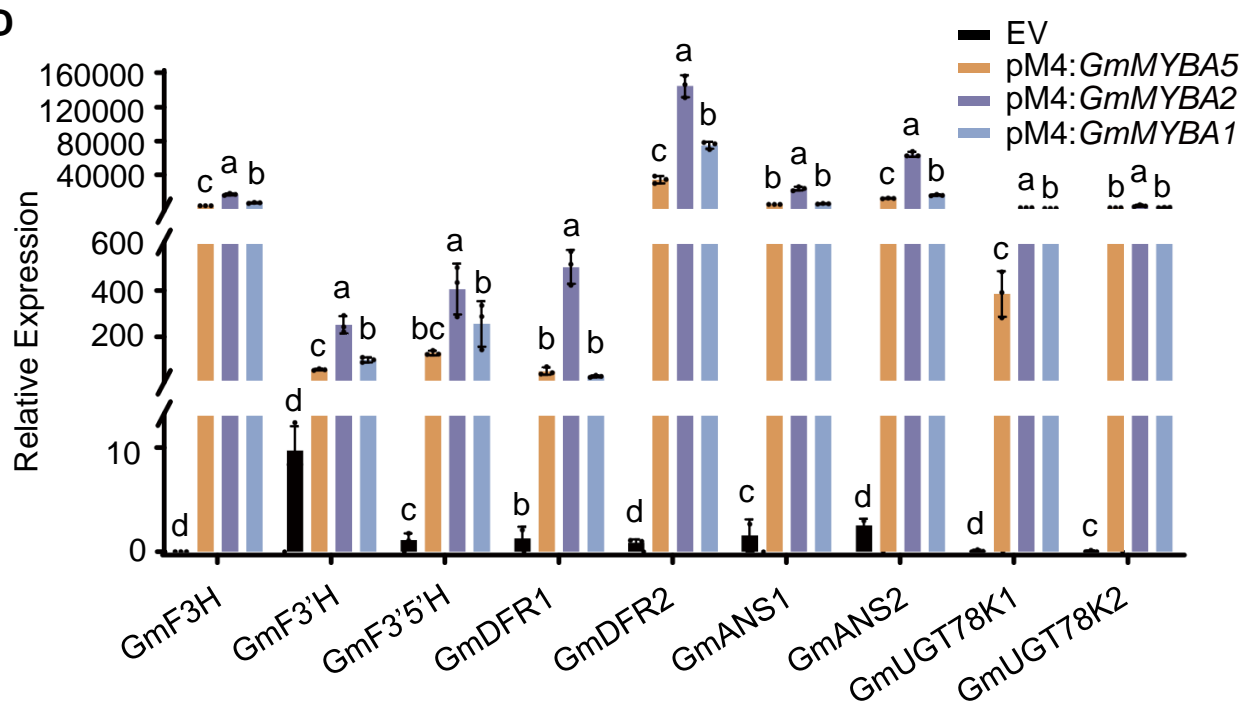
B



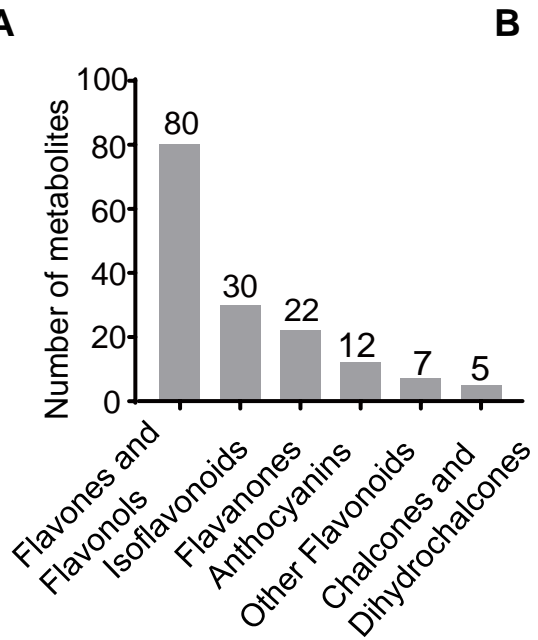
C



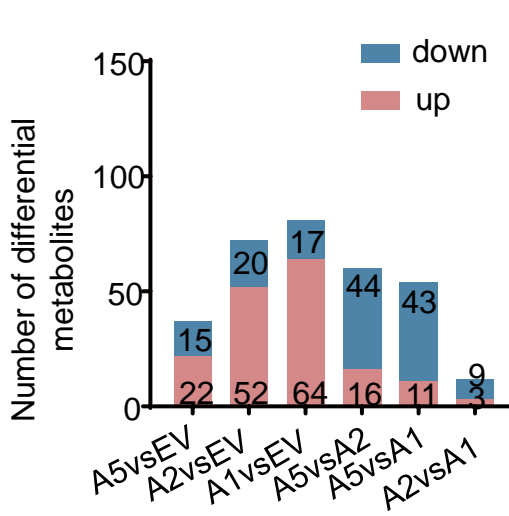
D



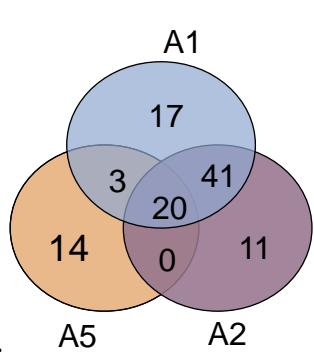
A



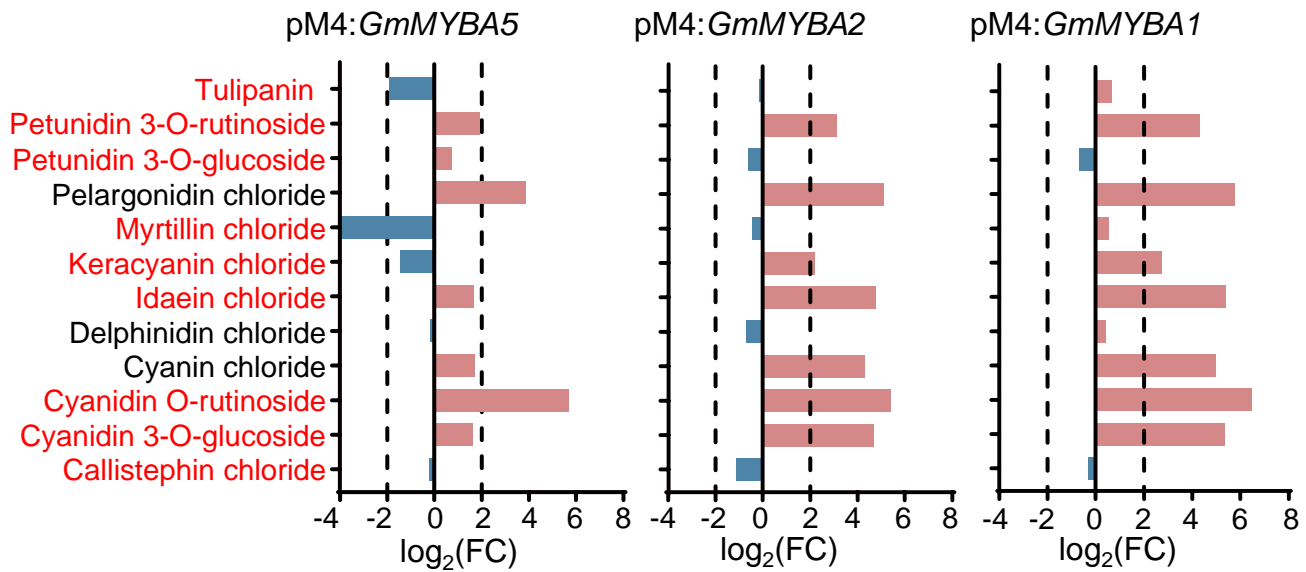
B

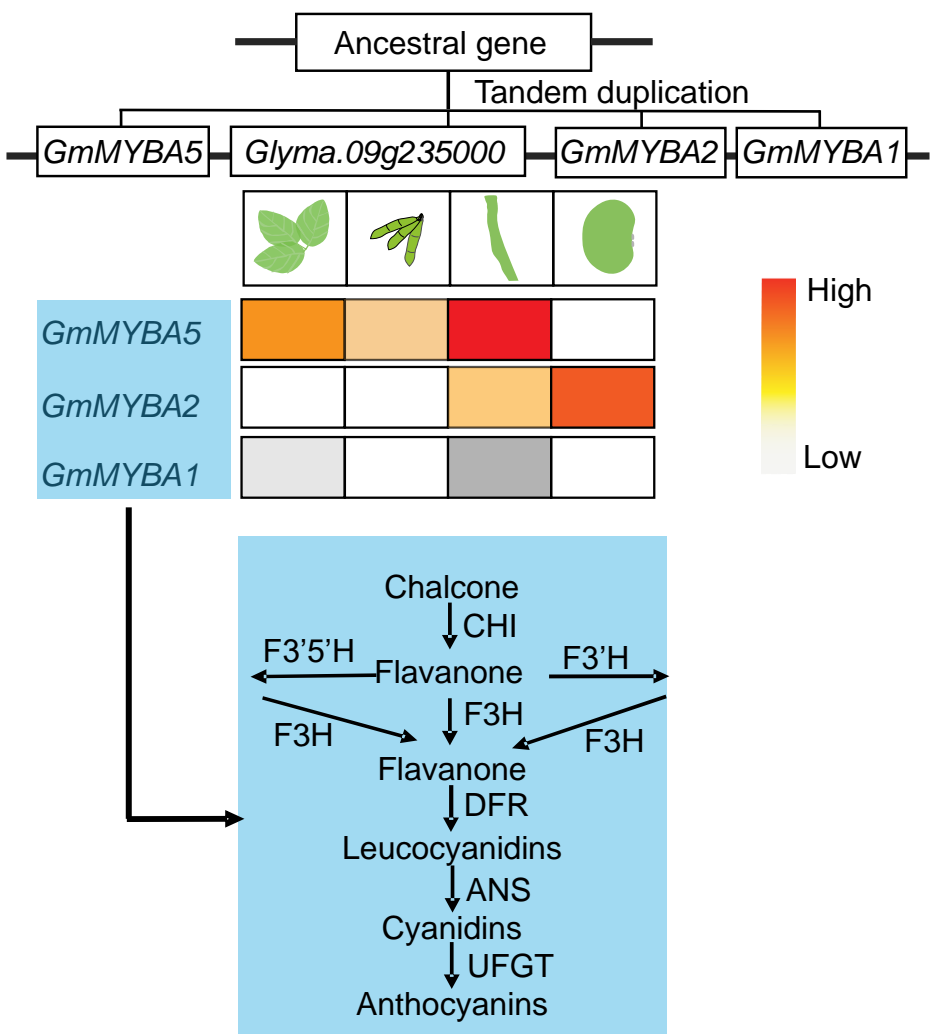


C



D





Parsed Citations

Albert NW, Davies KM, Lewis DH, Zhang H, Montefiori M, Brendolise C, Boase MR, Ngo H, Jameson PE, Schwinn KE. A conserved network of transcriptional activators and repressors regulates anthocyanin pigmentation in eudicots. *Plant Cell*, 2014;26(3):962-980. <https://doi.org/10.1105/tpc.113.122069>
Google Scholar: [Author Only](#) [Title Only](#) [Author and Title](#)

Bent A. *Arabidopsis thaliana* floral dip transformation method. *Methods Mol Biol*, 2006;343:87-103. <https://doi.org/10.1385/1-59745-130-4:87>
Google Scholar: [Author Only](#) [Title Only](#) [Author and Title](#)

Birchler JA, Veitia RA. One hundred years of gene balance: how stoichiometric issues affect gene expression, genome evolution, and quantitative traits. *Cytogenet Genome Res*, 2021;161(10-11):529-550. <https://doi.org/10.1159/000519592>
Google Scholar: [Author Only](#) [Title Only](#) [Author and Title](#)

Brown CJ, Todd KM, Rosenzweig RF. Multiple duplications of yeast hexose transport genes in response to selection in a glucose-limited environment. *Mol Biol Evol*, 1998;15(8):931-942. <https://doi.org/10.1093/oxfordjournals.molbev.a026009>
Google Scholar: [Author Only](#) [Title Only](#) [Author and Title](#)

Chen C, Liu XQ, Li SZ, Liu CX, Zhang YL, Luo LL, Miao LQ, Yang WZ, Xiao ZJ, Zhong Y, et al. Co-expression of transcription factors ZmC1 and ZmR2 establishes an efficient and accurate haploid embryo identification system in maize. *Plant J*, 2022a;111(5):1296-1307. <https://doi.org/10.1111/tpj.15888>
Google Scholar: [Author Only](#) [Title Only](#) [Author and Title](#)

Chen Y, Fang T, Su H, Duan SF, Ma RR, Wang P, Wu L, Sun WB, Hu QC, Zhao MX, et al. A reference-grade genome assembly for *Astragalus mongolicus* and insights into the biosynthesis and high accumulation of triterpenoids and flavonoids in its roots. *Plant Commun*, 2022b;4:100469. <https://doi.org/10.1016/j.xplc.2022.100469>
Google Scholar: [Author Only](#) [Title Only](#) [Author and Title](#)

Chin HS, Wu YP, Hour AL, Hong CY, Lin YR. Genetic and evolutionary analysis of purple leaf sheath in rice. *Rice*, 2016;9:8. <https://doi.org/10.1186/s12284-016-0080-y>
Google Scholar: [Author Only](#) [Title Only](#) [Author and Title](#)

D'Amelia V, Aversano R, Ruggiero A, Batelli G, Appelhagen I, Dinacci C, Hill L, Martin C, Carputo D. Subfunctionalization of duplicate MYB genes in *Solanum commersonii* generated the cold-induced ScAN2 and the anthocyanin regulator ScAN1. *Plant Cell and Environ*, 2018; 41(5):1038-1051. <https://doi.org/10.1111/pce.12966>
Google Scholar: [Author Only](#) [Title Only](#) [Author and Title](#)

Freeling M. Bias in plant gene content following different sorts of duplication: tandem, whole-genome, segmental, or by transposition. *Annu Rev of Plant Biol*, 2009;60:433-453. <https://doi.org/10.1146/annurev.arplant.043008.092122>
Google Scholar: [Author Only](#) [Title Only](#) [Author and Title](#)

Gao RF, Han TT, Xun HW, Zeng XS, Li PH, Li YQ, Wang YN, Shao Y, Cheng X, Feng XZ, et al. MYB transcription factors GmMYBA2 and GmMYBR function in a feedback loop to control pigmentation of seed coat in soybean. *J Exp Bot*, 2021;72(12):4401-4418. <https://doi.org/10.1093/jxb/erab152>
Google Scholar: [Author Only](#) [Title Only](#) [Author and Title](#)

García-Fernández C, Campa A, Ferreira JJ. Dissecting the genetic control of seed coat color in a RIL population of common bean (*Phaseolus vulgaris* L.). *Theor and Appl Genet*, 2021;134(11):3687-3698. <https://doi.org/10.1007/s00122-021-03922-y>
Google Scholar: [Author Only](#) [Title Only](#) [Author and Title](#)

Gietz RD, Schiestl RH. High-efficiency yeast transformation using the LiAc/SS carrier DNA/PEG method. *Nat Protoc*, 2007;2(1):31-34. <https://doi.org/10.1038/nprot.2007.13>
Google Scholar: [Author Only](#) [Title Only](#) [Author and Title](#)

Gillman JD, Tetlow A, Lee JD, Shannon JG, Bilyeu K. Loss-of-function mutations affecting a specific *Glycine max* R2R3 MYB transcription factor result in brown hilum and brown seed coats. *BMC Plant Biol*, 2011;11:155 <https://doi.org/10.1186/1471-2229-11-155>
Google Scholar: [Author Only](#) [Title Only](#) [Author and Title](#)

Gould KS. Nature's Swiss Army Knife: The diverse protective roles of anthocyanins in leaves. *J of Biomed and Biotechnol*, 2004;2004(5):314-320. <https://doi.org/10.1155/S1110724304406147>
Google Scholar: [Author Only](#) [Title Only](#) [Author and Title](#)

Grotewold E, Drummond BJ, Bowen B, Peterson T. The MYB-homologous p-gene controls phlobaphene pigmentation in maize floral organs by directly activating a flavonoid biosynthetic gene subset. *Cell*, 1994;76(3):543-553. [https://doi.org/10.1016/0092-8674\(94\)90117-1](https://doi.org/10.1016/0092-8674(94)90117-1)
Google Scholar: [Author Only](#) [Title Only](#) [Author and Title](#)

Guo WB, Zhao J, Li XX, Qin L, Yan XL, Liao H. A soybean β -expansin gene GmEXPB2 intrinsically involved in root system

architecture responses to abiotic stresses. *Plant J*, 2011;66(3):541-552. <https://doi.org/10.1111/j.1365-313X.2011.04511.x>

Google Scholar: [Author Only](#) [Title Only](#) [Author and Title](#)

Hastings PJ. Adaptive amplification. *Crit Rev Biochem and Mol Biol*, 2007;42(4):271-283. <https://doi.org/10.1080/10409230701507757>

Google Scholar: [Author Only](#) [Title Only](#) [Author and Title](#)

Herniter IA, Muñoz-Amatriaín M, Lo S, Guo YN, Close TJ. Identification of candidate genes controlling black seed coat and pod tip color in cowpea (*Vigna unguiculata* [L.] Walp). *G3 (Bethesda)*, 2018;8(10):3347-3355. <https://doi.org/10.1534/g3.118.200521>

Google Scholar: [Author Only](#) [Title Only](#) [Author and Title](#)

Hichri I, Barrieu F, Bogs J, Kappel C, Delrot S, Lauvergeat V. Recent advances in the transcriptional regulation of the flavonoid biosynthetic pathway. *J Exp Bot*, 2011;62(8):2465-2483. <https://doi.org/10.1093/jxb/erq442>

Google Scholar: [Author Only](#) [Title Only](#) [Author and Title](#)

Hou JJ, Fan WW, Ma RR, Li B, Yuan ZH, Huang WX, Wu YY, Hu Q, Lin CJ, Zhao XQ, et al. MALE STERILITY 3 encodes a plant homeodomain-finger protein for male fertility in soybean. *J Integr Plant Biol*, 2022;64(5):1076-1086. <https://doi.org/10.1111/jipb.13242>

Google Scholar: [Author Only](#) [Title Only](#) [Author and Title](#)

Huang D, Wang X, Tang ZZ, Yuan Y, Xu YT, He JX, Jiang XL, Peng SA, Li L, Butelli E, et al. Subfunctionalization of the Ruby2-Ruby1 gene cluster during the domestication of citrus. *Nat Plants*, 2018;4(11):930-941. <https://doi.org/10.1038/s41477-018-0287-6>

Google Scholar: [Author Only](#) [Title Only](#) [Author and Title](#)

Huang T, Xin S, Fang Y, Chen T, Chang J, Ko N, Huang H, Hua Y. Use of a novel R2R3-MYB transcriptional activator of anthocyanin biosynthesis as visual selection marker for rubber tree (*Hevea brasiliensis*) transformation. *Ind Crop and Prod*, 2021;174:114225. <https://doi.org/10.1016/j.indcrop.2021.114225>

Google Scholar: [Author Only](#) [Title Only](#) [Author and Title](#)

Innes RW, Ameline-Torregrosa C, Ashfield T, Cannon E, Cannon SB, Chacko B, Chen NW, Couloux A, Dalwani A, Denny R, et al. Differential accumulation of retroelements and diversification of NB-LRR disease resistance genes in duplicated regions following polyploidy in the ancestor of soybean. *Plant Physiology*, 2008;148(4):1740-1759. <https://doi.org/10.1104/pp.108.127902>

Google Scholar: [Author Only](#) [Title Only](#) [Author and Title](#)

James TC, Usher J, Campbell S, Bond U. Lager yeasts possess dynamic genomes that undergo rearrangements and gene amplification in response to stress. *Curr Genet*, 2008;53(3):139-152. <https://doi.org/10.1007/s00294-007-0172-8>

Google Scholar: [Author Only](#) [Title Only](#) [Author and Title](#)

Jeong SC, Moon JK, Park SK, Kim MS, Lee K, Lee SR, Jeong N, Choi MS, Kim N, Kang ST, et al. Genetic diversity patterns and domestication origin of soybean. *Theor Appl Genet*, 2019;132(4):1179-1193. <https://doi.org/10.1007/s00122-018-3271-7>

Google Scholar: [Author Only](#) [Title Only](#) [Author and Title](#)

Kereszt A, Li D, Indrasumunar A, Nguyen CD, Nontachaiyapoom S, Kinkema M, Gresshoff PM. Agrobacterium rhizogenes-mediated transformation of soybean to study root biology. *Nat Protoc*, 2007;2(4):948-952. <https://doi.org/10.1038/nprot.2007.141>

Google Scholar: [Author Only](#) [Title Only](#) [Author and Title](#)

Kim MY, Van K, Kang YJ, Kim KH, Lee SH. Tracing soybean domestication history: From nucleotide to genome. *Breeding Sci*, 2012;61(5):445-452. <https://doi.org/10.1270/jsbbs.61.445>

Google Scholar: [Author Only](#) [Title Only](#) [Author and Title](#)

Kovinich N, Kayanja G, Chanoca A, Otegui MS, Grotewold E. Abiotic stresses induce different localizations of anthocyanins in *Arabidopsis*. *Plant Signal Behav*, 2015;10(7):1027850. <https://doi.org/10.1080/15592324.2015.1027850>

Google Scholar: [Author Only](#) [Title Only](#) [Author and Title](#)

Li CX, Yu WJ, Xu JR, Lu XF, Liu YZ. Anthocyanin biosynthesis induced by MYB transcription factors in plants. *Int J Mol Sci*, 2022a;23(19):11701. <https://doi.org/10.3390/ijms231911701>

Google Scholar: [Author Only](#) [Title Only](#) [Author and Title](#)

Li Y, Fang XJ, Lin ZW. Convergent loss of anthocyanin pigments is controlled by the same MYB gene in cereals. *J Exp Bot*, 2022b;73(18):6089-6102. <https://doi.org/10.1093/jxb/erac270>

Li YH, Guan RX, Liu ZX, Ma YS, Wang LX, Li LH, Lin FY, Luan WJ, Chen PY, Yan Z, et al. Genetic structure and diversity of cultivated soybean (*Glycine max* (L.) Merr.) landraces in China. *Theor Appl Genet*, 2008;117(6):857-871. <https://doi.org/10.1007/s00122-008-0825-0>

Google Scholar: [Author Only](#) [Title Only](#) [Author and Title](#)

Lim SH, Kim DH, Cho MC, Lee JY. Chili Pepper AN2 (CaAN2): A visible selection marker for nondestructive monitoring of transgenic plants. *Plants (Basel)*, 2022;11(6):820. <https://doi.org/10.3390/plants11060820>

Google Scholar: [Author Only](#) [Title Only](#) [Author and Title](#)

Liu JY, Osbourn A, Ma PD. MYB Transcription Factors as Regulators of Phenylpropanoid Metabolism in Plants. *Mol Plant*,

2015;8(5):689-708. <https://doi.org/10.1016/j.molp.2015.03.012>

Google Scholar: [Author Only](#) [Title Only](#) [Author and Title](#)

Lloyd A, Brockman A, Aguirre L, Campbell A, Bean A, Cantero A, Gonzalez A. Advances in the MYB-bHLH-WD Repeat (MBW) pigment regulatory model: Addition of a WRKY factor and co-option of an anthocyanin MYB for betalain regulation. *Plant and Cell Physiol*, 2017; 58(9):1431-1441. <https://doi.org/10.1093/pcp/pcx075>

Google Scholar: [Author Only](#) [Title Only](#) [Author and Title](#)

Lu N, Rao X, Li Y, Jun JH, Dixon RA. Dissecting the transcriptional regulation of proanthocyanidin and anthocyanin biosynthesis in soybean (*Glycine max*). *Plant Biotechnol J*, 2021;19(7):1429-1442. <https://doi.org/10.1111/pbi.13562>

Google Scholar: [Author Only](#) [Title Only](#) [Author and Title](#)

Magadum S, Banerjee U, Murugan P, Gangapur D, Ravikesavan R. Gene duplication as a major force in evolution. *J Genet*, 2013;92(1):155-161. <https://doi.org/10.1007/s12041-013-0212-8>

Google Scholar: [Author Only](#) [Title Only](#) [Author and Title](#)

Malle S, Morrison M, Belzile F. Identification of loci controlling mineral element concentration in soybean seeds. *BMC Plant Biol*, 2020;20(1):419. <https://doi.org/10.1186/s12870-020-02631-w>

Google Scholar: [Author Only](#) [Title Only](#) [Author and Title](#)

Meyers BC, Kozik A, Griego A, Kuang H, Michelmore RW. Genome-wide analysis of NBS-LRR-encoding genes in *Arabidopsis*. *Plant Cell*, 2003;15(4):809-834. <https://doi.org/10.1105/tpc.009308>

Google Scholar: [Author Only](#) [Title Only](#) [Author and Title](#)

O'Neil J, Tchinda J, Gutierrez A, Moreau L, Maser RS, Wong KK, Li W, McKenna K, Liu XS, Feng B, et al. Alu elements mediate MYB gene tandem duplication in human T-ALL. *J Exp Med*, 2007;204(13):3059-3066. <https://doi.org/10.1084/jem.20071637>

Google Scholar: [Author Only](#) [Title Only](#) [Author and Title](#)

Putta S, Yarla NS, Peluso I, Tiwari DK, Reddy GV, Giri PV, Kumar N, Malla R, Rachel V, Bramhachari PV, et al. Anthocyanins: Multi-target agents for prevention and therapy of chronic diseases. *Cur Pharm Des*, 2017;23(41):6321-6346. <https://doi.org/10.2174/1381612823666170519151801>

Google Scholar: [Author Only](#) [Title Only](#) [Author and Title](#)

Riehle MM, Bennett AF, Long AD. Genetic architecture of thermal adaptation in *Escherichia coli*. *Proc Natl Acad Sci U S A*, 2001;98(2):525-530. <https://doi.org/10.1073/pnas.98.2.525>

Google Scholar: [Author Only](#) [Title Only](#) [Author and Title](#)

Rizzon C, Ponger L, Gaut BS. Striking similarities in the genomic distribution of tandemly arrayed genes in *Arabidopsis* and rice. *PLoS Comput Biol*, 2006;2(9):115. <https://doi.org/10.1371/journal.pcbi.0020115>

Google Scholar: [Author Only](#) [Title Only](#) [Author and Title](#)

Saigo T, Wang T, Watanabe M, Tohge T. Diversity of anthocyanin and proanthocyanin biosynthesis in land plants. *Curr Opin Plant Biol*, 2020;55:93-99. <https://doi.org/10.1016/j.pbi.2020.04.001>

Google Scholar: [Author Only](#) [Title Only](#) [Author and Title](#)

Sandve SR, Rohlfs RV, Hvidsten TR. Subfunctionalization versus neofunctionalization after whole-genome duplication. *Nat Genet*, 2018;50(7):908-909. <https://doi.org/10.1038/s41588-018-0162-4>

Google Scholar: [Author Only](#) [Title Only](#) [Author and Title](#)

Shin DH, Choi MG, Kang CS, Park CS, Choi SB, Park YI. A wheat R2R3-MYB protein PURPLE PLANT1 (TaPL1) functions as a positive regulator of anthocyanin biosynthesis. *Biochem Biophys Res Commun*, 2016;469(3):686-691. <https://doi.org/10.1016/j.bbrc.2015.12.001>

Google Scholar: [Author Only](#) [Title Only](#) [Author and Title](#)

Soltis PS, Marchant DB, Van de Peer Y, Soltis DE. Polyploidy and genome evolution in plants. *Curr Opin Genet Dev*, 2015;35:119-125. <https://doi.org/10.1016/j.gde.2015.11.003>

Google Scholar: [Author Only](#) [Title Only](#) [Author and Title](#)

Soltis PS, Soltis DE. Ancient WGD events as drivers of key innovations in angiosperms. *Curr Opin Plant Biol*, 2016;30:159-165. <https://doi.org/10.1016/j.pbi.2016.03.015>

Google Scholar: [Author Only](#) [Title Only](#) [Author and Title](#)

Stracke R, Werber M, Weisshaar B. The R2R3-MYB gene family in *Arabidopsis thaliana*. *Curr Opin Plant Biol*, 2001;4(5):447-456. [https://doi.org/10.1016/s1369-5266\(00\)00199-0](https://doi.org/10.1016/s1369-5266(00)00199-0)

Google Scholar: [Author Only](#) [Title Only](#) [Author and Title](#)

Sundaramoorthy J, Park GT, Lee JD, Kim JH, Seo HS, Song JT. Genetic and molecular regulation of flower pigmentation in soybean. *J KOREAN SOC APPL BI*, 2015; 58(4):555-562. <https://doi.org/10.1007/s13765-015-0077-z>

Google Scholar: [Author Only](#) [Title Only](#) [Author and Title](#)

Thompson JD, Higgins DG, Gibson TJ. CLUSTAL W: Improving the sensitivity of progressive multiple sequence alignment through sequence weighting, position-specific gap penalties and weight matrix choice. Nucleic Acids Res, 1994;22(22):4673-4680.
<https://doi.org/10.1093/nar/22.22.4673>
Google Scholar: [Author Only](#) [Title Only](#) [Author and Title](#)

Wang CN, Ji WK, Liu YC, Zhou P, Meng YY, Zhang PC, Wen JQ, Mysore KS, Zhai JX, Young ND, et al. The antagonistic MYB paralogs RH1 and RH2 govern anthocyanin leaf markings in *Medicago truncatula*. New Phytol, 2021;229(6):3330-3344.
<https://doi.org/10.1111/nph.17097>
Google Scholar: [Author Only](#) [Title Only](#) [Author and Title](#)

Wang JP, Sun PC, Li YX, Liu YZ, Yu JG, Ma XL, Sun SR, Yang NS, Xia RY, Lei TY, et al. Hierarchically aligning 10 legume genomes establishes a family-level genomics platform. Plant Physiol, 2017;174(1):284-300. <https://doi.org/10.1104/pp.16.01981>.
Google Scholar: [Author Only](#) [Title Only](#) [Author and Title](#)

Wang S, Xu Z, Yang Y, Ren W, Fang J, Wan L. Genome-wide analysis of R2R3-MYB genes in cultivated peanut (*Arachis hypogaea* L.): Gene duplications, functional conservation, and diversification. Front Plant Sci, 2023;14:1102174 <https://doi.org/1102174.10.3389/fpls.2023.1102174>
Google Scholar: [Author Only](#) [Title Only](#) [Author and Title](#)

Wang XP, Wang W, Chen SY, Lian YJ, Wang SC. *Tropaeolum majus* R2R3 MYB transcription factor TmPAP2 functions as a positive regulator of anthocyanin biosynthesis. Int J Mol Sci, 2022;23(20):12395. <https://doi.org/10.3390/ijms232012395>
Google Scholar: [Author Only](#) [Title Only](#) [Author and Title](#)

Xie M, Chung CY, Li MW, Wong FL, Wang X, Liu A, Wang Z, Leung AK, Wong TH, Tong SW, et al. A reference-grade wild soybean genome. Nat Commun, 2019;10(1):1216. <https://doi.org/10.1038/s41467-019-09142-9>
Google Scholar: [Author Only](#) [Title Only](#) [Author and Title](#)

Xu WJ, Dubos C, Lepiniec, L. Transcriptional control of flavonoid biosynthesis by MYB-bHLH-WDR complexes. Trends in Plant Sci, 2015;20(3):176-185. <https://doi.org/10.1016/j.tplants.2014.12.001>
Google Scholar: [Author Only](#) [Title Only](#) [Author and Title](#)

Yang ZH. PAML 4: phylogenetic analysis by maximum likelihood. Mol Biol Evol, 2007;24(8):1586-1591.
<https://doi.org/10.1093/molbev/msm088>
Google Scholar: [Author Only](#) [Title Only](#) [Author and Title](#)

Yin LW, Xu G, Yang JL, Zhao MX. The heterogeneity in the landscape of gene dominance in maize is accompanied by unique chromatin environments. Mol Biol Evol, 2022;39(10). <https://doi.org/10.1093/molbev/msac198>
Google Scholar: [Author Only](#) [Title Only](#) [Author and Title](#)

Zabala G, Vodkin LO. Methylation affects transposition and splicing of a large CACTA transposon from a MYB transcription factor regulating anthocyanin synthase genes in soybean seed coats. PLoS One, 2014;9(11):111959.
<https://doi.org/10.1371/journal.pone.0111959>
Google Scholar: [Author Only](#) [Title Only](#) [Author and Title](#)

Zhang H, Zhang F, Yu YM, Feng L, Jia JB, Liu B, Li BS, Guo HW, Zhai JX. A comprehensive online database for exploring ~20,000 public *Arabidopsis* RNA-seq libraries. Mol Plant, 2020;13(9):1231-1233. <https://doi.org/10.1016/j.molp.2020.08.001>
Google Scholar: [Author Only](#) [Title Only](#) [Author and Title](#)

Zhang N, McHale LK, Finer JJ. Isolation and characterization of "GmScream" promoters that regulate highly expressing soybean (*Glycine max*. Merr.) genes. Plant Sci, 2015;241:189-198. <https://doi.org/10.1016/j.plantsci.2015.10.010>
Google Scholar: [Author Only](#) [Title Only](#) [Author and Title](#)

Zhang P, Chopra S, Peterson T. A segmental gene duplication generated differentially expressed myb-homologous genes in maize. Plant Cell, 2000;12(12):2311-2322. <https://doi.org/10.1105/tpc.12.12.2311>
Google Scholar: [Author Only](#) [Title Only](#) [Author and Title](#)

Zhang SL, Kondorosi É, Kereszt A. An anthocyanin marker for direct visualization of plant transformation and its use to study nitrogen-fixing nodule development. J Plant Res, 2019;132(5):695-703. <https://doi.org/10.1007/s10265-019-01126-6>
Google Scholar: [Author Only](#) [Title Only](#) [Author and Title](#)

Zhang Y, Butelli E, Martin C. Engineering anthocyanin biosynthesis in plants. Curr Opin Plant Biol, 2014;19:81-90.
<https://doi.org/10.1016/j.pbi.2014.05.011>
Google Scholar: [Author Only](#) [Title Only](#) [Author and Title](#)

Zhao MX, Zhang B, Lisch D, Ma JX. Patterns and consequences of subgenome differentiation provide insights into the nature of paleopolyploidy in plants. Plant Cell, 2017;29(12):2974-2994. <https://doi.org/10.1105/tpc.17.00595>
Google Scholar: [Author Only](#) [Title Only](#) [Author and Title](#)